

**MEASURING VEGETATION HEALTH USING  
GROUND PENETRATING RADAR AND ITS  
CORRELATION WITH DATA FROM SPECTRAL  
RADIOMETER**

by

Maritza Torres Candelaria

A thesis submitted in partial fulfillment of the requirements for the degree of

MASTER OF SCIENCE  
in  
ELECTRICAL ENGINEERING  
(Applied Electromagnetics)

UNIVERSITY OF PUERTO RICO  
MAYAGÜEZ CAMPUS  
2005

Approved by:

\_\_\_\_\_  
Mario Ierkic, PhD  
Member, Graduate Committee

\_\_\_\_\_  
Date

\_\_\_\_\_  
Ramón Vazquez, PhD  
Member, Graduate Committee

\_\_\_\_\_  
Date

\_\_\_\_\_  
Hamed Parsiani, PhD  
President, Graduate Committee

\_\_\_\_\_  
Date

\_\_\_\_\_  
Eric Harmsen, PhD  
Representative of Graduate Studies

\_\_\_\_\_  
Date

\_\_\_\_\_  
Isidoro Couvertier, PhD  
Chairperson of the Department

\_\_\_\_\_  
Date

## ABSTRACT

Changes in vegetation can affect our health, the environment and the economy. Understanding this, twenty years ago scientists began to use satellite remote sensors to monitor major fluctuations in vegetation and understand how it affects the environment. Previous work was done using passive sensors and the Normalized Difference Vegetation Index (NDVI), with 1 km<sup>2</sup> satellite resolution. In this research the emphasis has been to calculate vegetation health using active sensors such as radar, which dominates a very fine resolution. Wideband radar, Ground Penetrating Radar (GPR), with range from 300MHz to 3GHz with center frequency of 1.5GHz has been implemented obtaining multiple responses for vegetation at various wavelengths. Materials Characteristics in Fourier Domain (MCFD) was developed and its power at multiple wavelengths of the wide-band radar has shown to be a good indicator of vegetation health. The GPR and NDVI values compared favorably with a correlation of -0.97.

## RESUMEN

Los cambios que sufre la vegetación afectan la salud, el ambiente y la economía. Conscientes de esta realidad, los científicos de hace veinte años comenzaron a utilizar sensores remotos ubicados en los satélites que orbitan el planeta para detectar cambios y fluctuaciones en la salud de la vegetación con el propósito de entender cómo estos cambios afectan el ambiente. En el pasado, se utilizaron sensores pasivos y el Índice Normalizado de Diferencia en la Vegetación (conocido como NDVI por sus siglas en inglés), con una resolución vía satélite de  $1\text{Km}^2$  para llevar a cabo estas investigaciones. El énfasis de esta investigación fue poder calcular la salud de la vegetación usando sensores activos como el radar, donde domina una alta resolución. El radar de banda ancha, tal como el Radar de Penetración de la Terreno (GPR, por sus siglas en inglés), con un rango que va desde 300MHz a 3GHz con una frecuencia de centro de 1.5GHz ha sido implementado obteniendo múltiples respuestas respecto a la vegetación, a varios largos de onda. Las Características de Materiales en el Dominio de Fourier (conocido como MCFD, por sus siglas en inglés) fue desarrollada en la investigación y su potencia acumulada en múltiples largos de onda del radar de banda ancha demostraron ser un buen indicador de la salud de la vegetación. Los valores obtenidos con el GPR y el NDVI compararon favorablemente ya que hubo una correlación de -0.97.

© MARITZA TORRES CANDELARIA, 2005

## ACKNOWLEDGEMENTS

During the development of my graduate studies in the University of Puerto Rico several persons collaborated directly and indirectly with my research. Without their support it would be impossible for me to finish my work. That is why I wish to dedicate this section to recognize their support.

*To Professor Hamed Parsiani:* Thank you for the opportunity to research under your guidance and supervision; and for your dedication in this project.

*To Professors Mario Ierkic and Ramón Vazquez:* Thank you for being part of my committee and for going out of your way in order to make this possible.

*To Professor Pérez Alegría:* Thank you for your patience in lending the spectrometer for so long in order to make possible this experiment.

*To my family:* Thank you for your support in every goal I've set for myself; specially my mother for the foundation that you have given me, which has been the drive that I have had for pursuing my studies.

*To Alex:* Thank you for encouraging me into finishing this work, without you this would not have been possible.

I also want to thank God for his grace and love in permitting me to finish this achievement in my life.

The Grant from NOAA, NA17AE1625, provided the funding and the resources for the development of this research.

# Table of Contents

ABSTRACT .....	II
RESUMEN .....	III
© MARITZA TORRES CANDELARIA, 2005.....	IV
ACKNOWLEDGEMENTS .....	V
TABLE OF CONTENTS .....	VI
FIGURES LIST.....	VIII
TABLES LIST .....	X
<b>1 INTRODUCTION .....</b>	<b>1</b>
1.1 OBJECTIVES .....	3
1.2 LITERATURE REVIEW .....	3
1.3 SUMMARY OF FOLLOWING CHAPTERS .....	11
<b>2 THEORETICAL BACKGROUND.....</b>	<b>12</b>
2.1 NORMALIZED DIFFERENCE VEGETATION INDEX (NDVI).....	12
2.1.1 <i>Satellite Spectrometers</i> .....	13
2.1.2 <i>Handheld Spectrometers</i> .....	14
2.2 GROUND PENETRATING RADAR (GPR).....	15
2.2.1 <i>Electromagnetic Background</i> .....	15
2.2.2 <i>Resolution</i> .....	16
2.2.3 <i>GPR Antennas</i> .....	20
2.2.4 <i>GPR Data Collection Terminology</i> .....	22
2.3 EQUIPMENT AND MATERIALS .....	23
2.3.1 <i>Ground Penetrating Radar (GPR)</i> .....	23
2.3.2 <i>Spectral Radiometer</i> .....	28
2.3.3 <i>Software Used</i> .....	28
2.3.4 <i>Plantain Leaves</i> .....	29
<b>3 EXPERIMENT SETUP AND METHODOLOGY .....</b>	<b>30</b>
3.1 DATA ACQUISITION.....	30
3.2 DATA ANALYSIS .....	31
<b>4 ACTIVE VEGETATION INDEX VS. NDVI.....</b>	<b>35</b>
4.1 FIRST SET.....	35
4.1.1 <i>Spectrometer Experiment</i> .....	35

4.1.2	<i>GPR Experiment</i> .....	37
4.2	SECOND SET.....	40
4.2.1	<i>Spectrometer Experiment</i> .....	40
4.2.2	<i>GPR Experiment</i> .....	41
4.3	COMBINED RESULTS .....	45
5	CONCLUSIONS AND FUTURE WORK .....	47
APPENDIX A	MATLAB CODE FOR MCFD .....	50
APPENDIX B	DATA FROM SPECTROMETER.....	52

# Figures List

Figures	Page
Figure 1-1 CC vs. NDVI.....	4
Figure 1-2 CC vs. NDVI for Forest.....	5
Figure 1-3 Seasonal Change of Mean Values of NDVI.....	6
Figure 1-4 Seasonal Change of Mean value of SAR CCT counts.....	6
Figure 1-5 Leaf Structure Diagram.....	8
Figure 1-6 NDVI example.....	10
Figure 2-1 Typical Leaf Spectral Signature [6].....	12
Figure 2-2 Permittivity vs. Gravimetric Moisture.....	16
Figure 2-3 Instantaneous Field of View (IFOV).....	18
Figure 2-4 Illustration of the geometrical instantaneous field-of-view reconstructed by projection from a pixel in the image plane.....	19
Figure 2-5 Spectral Resolution.....	20
Figure 2-6 Plot of sample scan line in air.....	21
Figure 2-7 Plot of sample scan line on top of a leaf.....	22
Figure 2-8 The GSSI SIR-20.....	23
Figure 2-9 The antenna (with housing) and its representation.....	24
Figure 2-10 GPR images taken both across and along track the antenna with a metal rod placed at different depths.....	26
Figure 2-11 The intensity distribution at the depth of two inches for TE mode.....	27
Figure 2-12 Radiation Pattern Across and Along Track.....	28
Figure 2-13 The FieldSpec Handheld Spectrometer.....	28
Figure 2-14 Vegetation Levels.....	29
Figure 3-1 Spectrometer Experiment Setup.....	30
Figure 3-2 Image obtained from GPR for leaf level #2 and the intensity of a scan line of vegetation and air represented in Matlab ®.....	31
Figure 3-3 System Representation of the layer characteristics, the transmitted and reflected waves. .....	33
Figure 3-4 System Representation for the new layer characteristics, the transmitted and reflected waves.....	33
Figure 3-5 Flowchart for Matlab Program.....	34
Figure 4-1 Spectrums of each level of health of the plantain leaves.....	36
Figure 4-2 Intensity Plot for Leaf Level #1.....	37
Figure 4-4 Intensity Plot for Leaf Level #2.....	37
Figure 4-5 MCFD for Leaf Level #2.....	37
Figure 4-6 Intensity Plot for Leaf Level #3.....	38
Figure 4-7 MCFD for Leaf Level #3.....	38
Figure 4-8 Intensity Plot for Leaf Level #4.....	38

Figure 4-9 MCFD for Leaf Level #4.....	38
Figure 4-10 Intensity Plot for Leaf Level #5 .....	39
Figure 4-11 MCFD for Leaf Level #5.....	39
Figure 4-12 Intensity Plot for Leaf Level #6 .....	39
Figure 4-13 MCFD for Leaf Level #6.....	39
Figure 4-14 Spectrums of each level of health of the banana leaves.....	40
Figure 4-15 Intensity Plot for Leaf Level #1 .....	41
Figure 4-16 MCFD for Leaf Level #1 .....	41
Figure 4-17 Intensity Plot for Leaf Level #2 .....	42
Figure 4-18 MCFD for Leaf Level #2.....	42
Figure 4-19 Intensity Plot for Leaf Level #3 .....	42
Figure 4-20 MCFD for Leaf Level #3.....	42
Figure 4-21 Intensity Plot for Leaf Level #4 .....	43
Figure 4-22 MCFD for Leaf Level #4.....	43
Figure 4-23 Intensity Plot for Leaf Level #5 .....	43
Figure 4-24 MCFD for Leaf Level #5.....	43
Figure 4-25 Intensity Plot for Leaf Level #6 .....	44
Figure 4-26 MCFD for Leaf Level #6.....	44
Figure 4-27 GPR-MCFD Power vs. NDVI.....	45

# Tables List

<b>Tables</b>	<b>Page</b>
TABLE 2-1 TM Data .....	27
TABLE 2-2 TE Data .....	27
TABLE 4-1 NDVI for each level.....	36
TABLE 4-2 Average Power for All Levels.....	40
TABLE 4-3 NDVI for each level.....	41
TABLE 4-4 Average Power for All Levels.....	44

---

# 1 INTRODUCTION

Vegetation plays an important role on earth; it serves as air purification filter, as food supply, material for cloths, etc. Therefore measuring vegetation health is very important. Changes in vegetation can affect our health, the environment and the economy. Understanding this, twenty years ago scientists began to use satellite remote sensors to monitor major fluctuations in vegetation and understand how it affects the environment. They defined vegetation index, in particular the Normalized Difference Vegetation Index (NDVI), which is measured using passive sensors (radiometers).

The vegetation index has been modified in many ways over the years, but still uses the same concept. It uses two bands, the red from the visible spectrum (600-700nm) and the Near Infrared (700-1100nm), for its calculation. The reason these bands are the ones used will be explained in section 2.1.2. A disadvantage of passive sensors is that the resolution achieved may not be compared to the resolution achieved with radar. Radiometers that are used now, like MODIS (Moderate Resolution Imaging Spectral Radiometer), have spatial resolutions in the order of kilometers. Radiometers depend on a light source and do not penetrate clouds. In areas like the tropics where there are a lot of cloud-covers, radiometers can't be so effective.

On the other hand active sensors provide their own source of energy. They are designed to illuminate a target with radiation and measure the reflected energy. Common active remote sensors are RADAR, SONAR, and LIDAR. RADAR is an acronym for **RA**dio **D**etection **A**nd **R**anging. The earliest radar systems operated in the radio band of the electromagnetic spectrum from approximately 1 to 10m. Modern radar systems

---

transmit in the shorter wavelength microwave band from approximately 0.8cm to 1m. A radar system produces frequent, short bursts of microwave energy and measures the strength of the reflected echo, sometimes referred to as backscatter. Longer-wavelength radar systems can penetrate clouds and some surfaces such as sand and snow. This makes it an ideal tool for imaging tropical regions that have almost constant cloud cover. It is possible to choose a wavelength that doesn't penetrate that much in vegetation but reflects on it. The results would be more accurate and precise, because the resolution of radar is very superior to that of remote radiometers. Satellite SAR's have resolution in the order of meters like the RADARSAT-2, which has a range resolution up to 3m.

Before using satellite radars directly, the first step is to measure vegetation health with closer radar, like the Ground Penetrating Radar (GPR) working in the L-band. The L-band is an appropriate range to choose since it has been proven in [1] to be sensitive to vegetation change. By using closer radar there is a better control of the factors that affects the measuring of vegetation health. Then this data can be used to verify data from aerial sensors, like ATLAS (Advanced Thermal and Land Applications Sensor), and finally satellites.

The data collected from the GPR is compared and correlated to a handheld spectrometer, instrument that is being used currently to measure NDVI. The handheld spectrometer is chosen because it measures the same area as the GPR. This project has attained the correlation between GPR and handheld spectrometer. This is an important achievement since a correlation was found between the vegetation backscattered radar signals and the NDVI.

---

## 1.1 Objectives

The objective of this project is to measure the vegetation health using an active sensor with very high resolution. The Ground Penetrating Radar will serve as the active sensor. The data obtained will be correlated with the data obtained by the passive sensor, the spectrometer. This will be done in order to obtain vegetation health results with high resolution (about 1 meter) of the vegetation health. The objectives include:

- Investigate current studies of vegetation health, using Spectrometers and Radars.
- Analyze different signatures of various types of vegetation using the Handheld Spectrometer.
- Calculate average power of the signal backscattered from the vegetation.
- Correlate data obtained from Spectrometer with the Average Power obtained from the GPR.
- Define an active vegetation index.

## 1.2 Literature Review

A study done in [2] found an inverse relationship between what is called coherence coefficient and NDVI. The coherence coefficient is obtained by a method called Synthetic Aperture Radar (SAR) interferometry. SAR records both amplitude and phase of the backscattered echoes, and for interferometry not only the amplitude of the signal is considered, but its phase as well. The technique consists of having two coincident SAR images with slightly different sensor positions and calculating the phase difference, the

---

visualization of these phase differences is called an interferogram and the difference value is called coherence coefficient (CC).

Two antennas may be mounted on one aircraft and form along-track interferometry or across-track interferometry. If only one antenna is used it is called repeat-pass interferometry, which is the normal implementation for satellite. The study was done using data from the ERS1 & 2 Tandem form 20th and 21st of May 1996, and ERS 1 & 2 Tandem form the 10th and 11th of October 1997, these were compared to Landsat TM from 18th of February 1997 which is geocoded. The study area was Mayon in the Alabay province of Philippines. The result is shown in figure 1.1, where an inverse linear relationship, with a correlation coefficient of  $-0.903$ , was found for NDVI greater than  $0.4$ , categorized as forests.

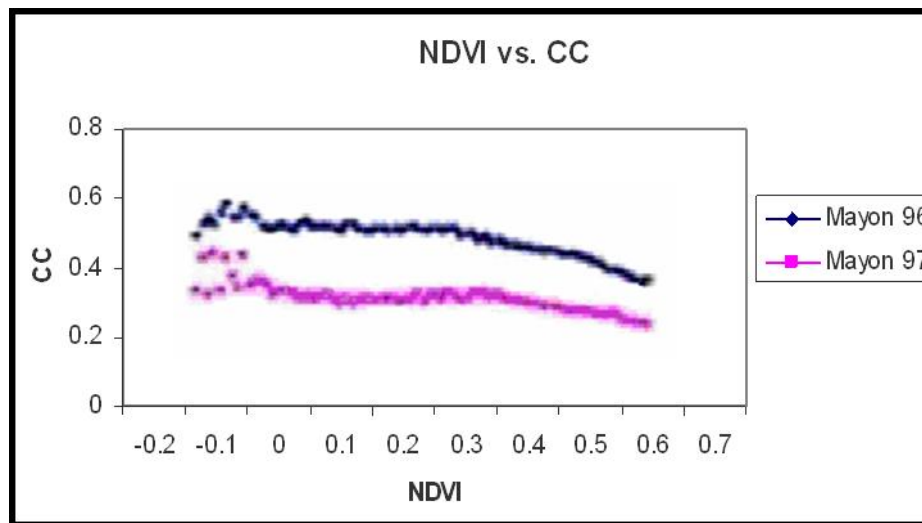


**Figure 1-1 CC vs. NDVI**

This research was expanded by [3] using the same instruments and the same study area, but concentrating on the relationship between CC and NDVI; specifically for NDVI greater than  $0.4$ . Wavelet filtering was applied on the raw data to eliminate noise and to

find a relationship. The correlation analysis between NDVI and both coherence data 1996 and 1997 also yields the correlation values of  $-0.93$  and  $-0.92$ , respectively. The linear fit of the data obtained is shown in Figure 1.2.

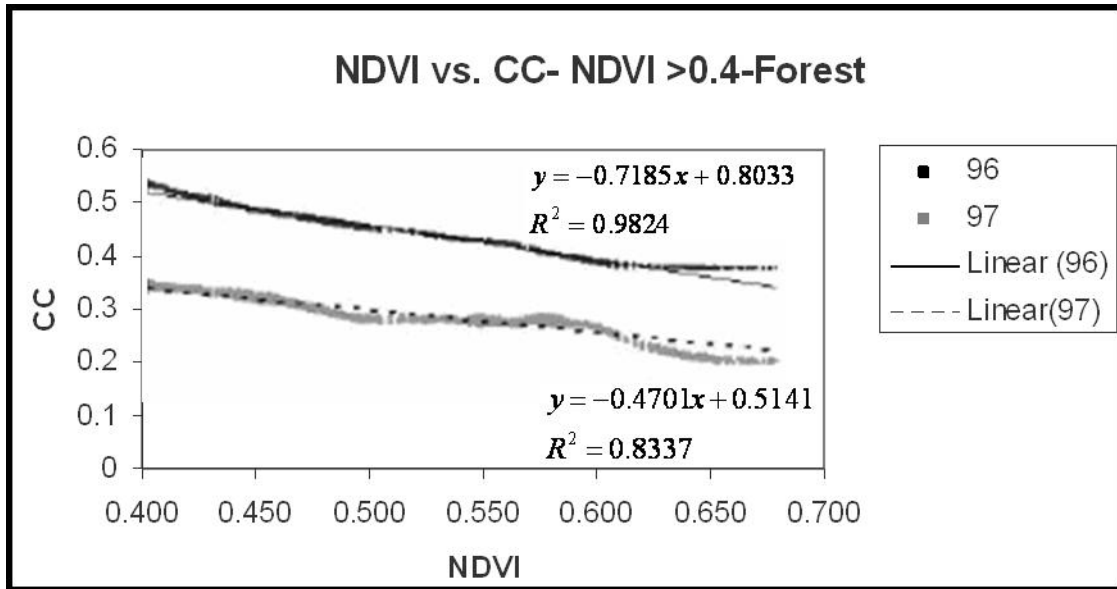


**Figure 1-2 CC vs. NDVI for Forest**

Another study was done in [4] comparing SAR coherence coefficient count using the JERS- with Landsat-5 TM. NDVI, the index in popular use, stands for amount and vigor of vegetation at the surface, which has relationship between amounts of accumulating biomass. SAR data has been used to get information about plant biomass from vast areas, therefore a relationship between NDVI to SAR CCT count is expected. The study related SAR data to NDVI by comparison of the two values on seasonal and annual changes in various forests in Kyoto City, Japan. The scenes selected were five scenes of Landsat TM acquired on: 08/06/96, 01/13/97, 08/25/97, 12/15/97, and 09/13/98; and five scenes of JERS-1 acquired on: 08/30/96, 01/9/97, 12/27/97, 05/8/98, and 06/21/98. The results

were not correlated, but plotted in two different plots. These plots are shown in figure 1.3 and 1.4.

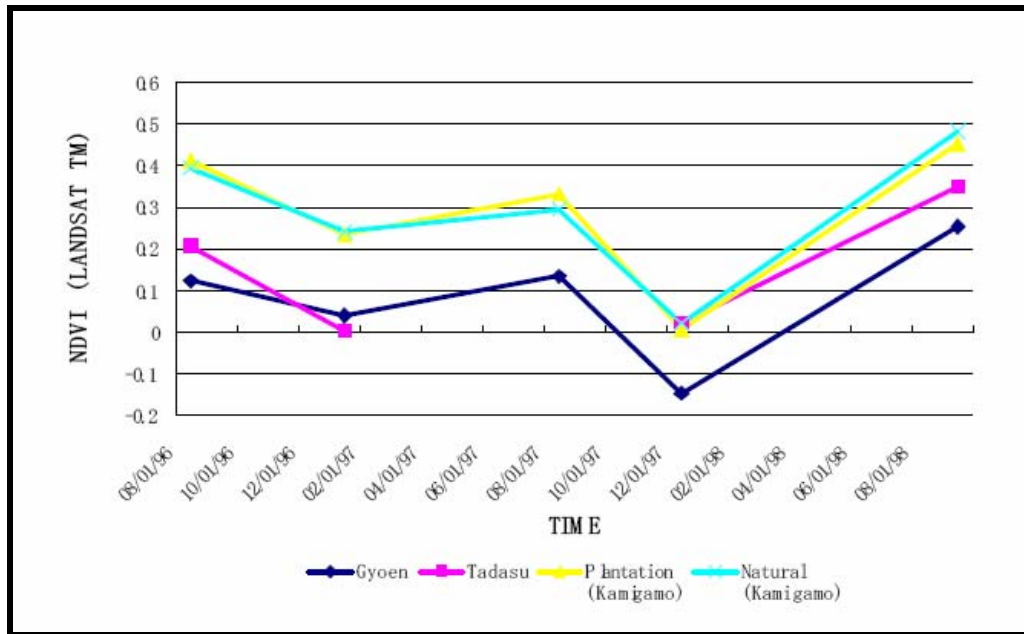


**Figure 1-3 Seasonal Change of Mean Values of NDVI**

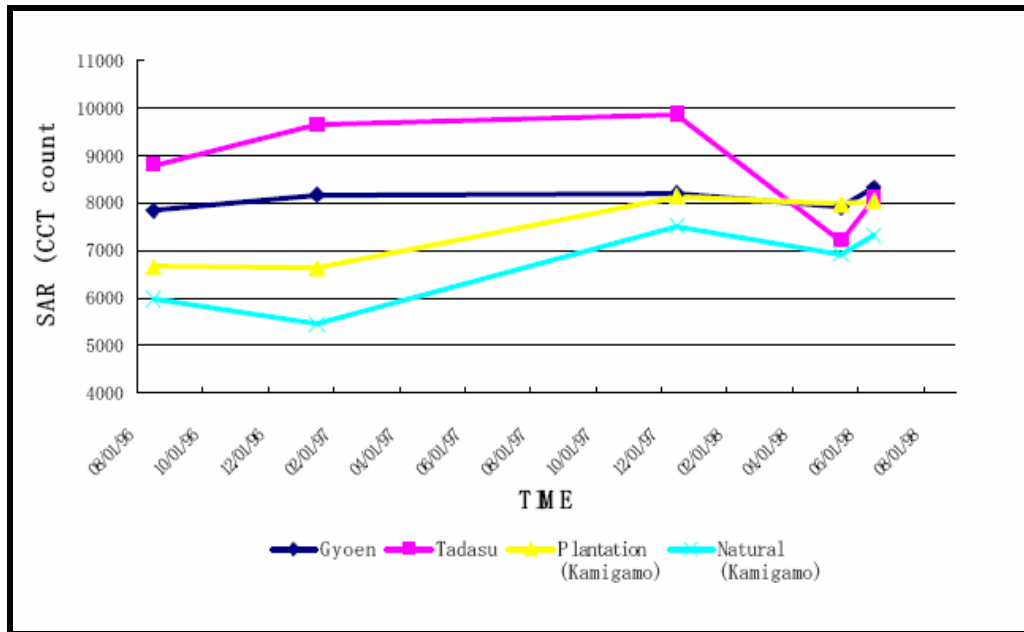
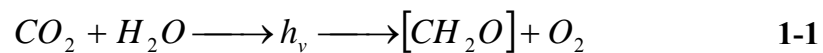


**Figure 1-4 Seasonal Change of Mean value of SAR CCT counts**

---

The plots show a trend in the relationship between SAR and NDVI. They found that the SAR CC changed as NDVI changed seasonally, they have an inverse relationship as NDVI decreased the SR CCT increased and vice versa. The resolution in this experiment was 30 m, for both active and passive sensors. This study is supported by the fact that electromagnetic radiation [5] and NDVI have been used as measures of biomass, and vegetation vigor, respectively.

Photosynthesis in terrestrial vegetation occurs in chloroplast organelles, contained in plant leaves [6]. The basic photosynthesis equation is:



Where  $CO_2$  and  $H_2O$  are combined, driven by light absorption to produce carbohydrates/sugars/etc.

The leaf structure allows for regular contact between atmosphere and the hydrated mesophyll cells (water) and provides the optical environment for incident photosynthetic active radiation (IPAR) interaction with chloroplast containing cells, shown in figure 1.5.

There are three main optical domains influencing the optical properties of plants, namely the visible region, the Near Infra Red (NIR), and the Middle-Infra Red (MIR). In the visible bands (0.4 to 0.7 $\mu$ m), light absorption by leaf pigments dominates the reflectance spectrum of the leaf and leads to generally lower reflectances (15% maximum). IPAR is absorbed strongly by plant pigments; chlorophyll a and chlorophyll b (60 to 75%), and carotenoids (25-35%).

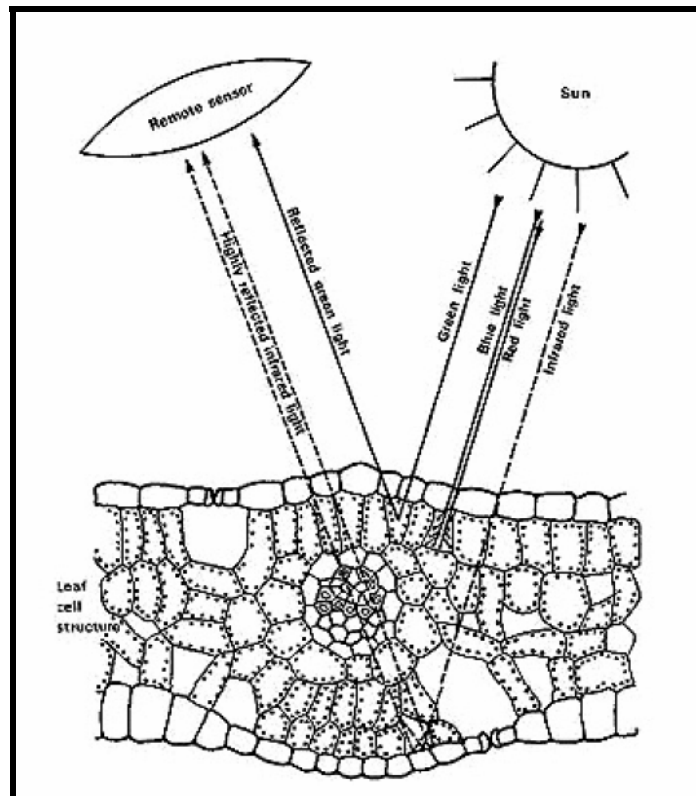


**Figure 1-5 Leaf Structure Diagram**

Absorption centered at about  $0.65\mu\text{m}$  (visible red) by chlorophyll pigment in green-leaf chloroplast that reside in the outer or Palisade leaf, and to a similar extent in the blue, removes these colors from white light, leaving the predominant but diminished reflectance for visible wavelengths concentrated in the green. Thus, most vegetation has a green-leafy color.

Other leaf pigments also have an important effect of the visible spectrum. For example, the yellow to orange-red pigment, the carotene, has a strong absorption in the  $0.35\text{-}0.50\mu\text{m}$  range and is responsible for the color of some flowers and fruits as well as of leaves without chlorophyll. Blue absorption is from carotenoid pigments which become pronounced as chlorophyll in the leaves decreases during senescence.

---

The red and blue pigment, xanthophyll, has strong absorption in the 0.35-0.50 $\mu\text{m}$  range and is responsible for the leaf color in fall.

In the near-infrared spectral domain (0.70-1.30  $\mu\text{m}$ ), leaf structure explains the optical properties. Two main spectral regions:

- Between 0.70 and 1.10  $\mu\text{m}$ , where reflectance is high due to spongy mesophyll cells, except in two minor water-related absorption bands (0.96 and 1.10  $\mu\text{m}$ ) and
- Between 1.10 and 1.30  $\mu\text{m}$ , which is the transition between the high NIR reflectances and the water-related absorption bands of the MIR.

Light reflects mainly at cell wall/air space interfaces, much of which emerges as strong reflection rays.

The last optical domain is the middle-infrared (1.30 -2.50  $\mu\text{m}$ ) characterized by the light absorption by the leaf water. Liquid water, which comprises 70-90% of the wet weight of leaves, strongly absorbs incident solar radiation in this range. This liquid water is transparent to the PAR wavelengths. Because water strongly absorbs radiation at 1.45 and 1.95  $\mu\text{m}$ , these wavelengths can not be used for reflectance measurements.

NDVI is an abbreviation for normalized difference vegetation index, a model for converting satellite-based measurements into surface vegetation types. The NDVI uses a complex ratio of reflectance in the red and near-infrared portions of the spectrum to accomplish this. Reflectance in the red region decreases with increasing chlorophyll content of the plant canopy, while reflectance in the infrared increases with increasing wet plant biomass. This technique has been used most successfully with data from the AVHRR, and is actually used operationally to predict the degree of drought and potential

famine in the Sahel region of Africa. It is a quantity that measures greenness and vigor of vegetation. AVHRR resolution is  $1\text{Km}^2$ , where one pixel represents an area of one kilometer. NDVI has a range from -1 to +1, a zero means no vegetation and any value close to +1(0.8-0.9) indicates the highest possible density of green leaves [7]. Figure 1.6 demonstrate how a lower NDVI (0.17) refers to an unhealthy tree, versus a higher NDVI (0.72) demonstrates a healthy tree. It may be seen that for the healthy plant there is a low reflection (high absorption) in the visible region and a high reflection in the NIR, while for the unhealthy one there is more reflection in the visible region (less absorption) than in the healthy one and also the NIR reflection is lower.

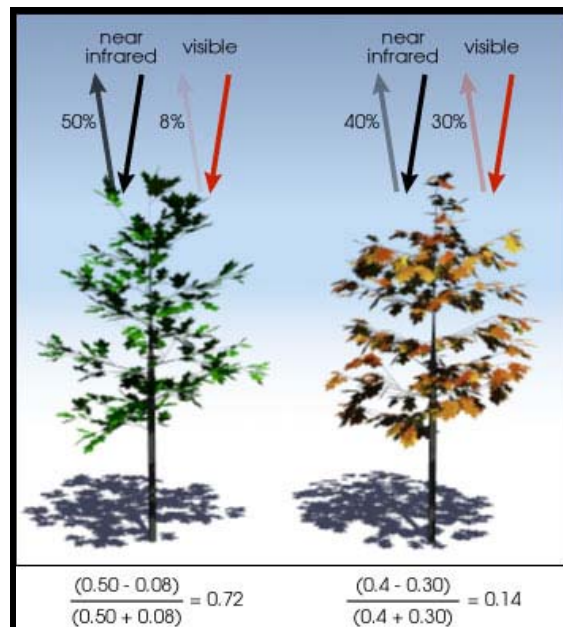


**Figure 1-6 NDVI example**

---

### **1.3 Summary of Following Chapters**

Chapter 2 deals with necessary background theory, the history and information about NDVI, electromagnetic theory, and the equipment used for the experiment. The third chapter presents the MCFD methodology and the experimental setup related to the comparison of NDVI and RADAR data. The data collected for the comparison and analysis are shown in Chapter 4. Finally conclusions and future work are presented in Chapter 5.

---

## 2 THEORETICAL BACKGROUND

### 2.1 Normalized Difference Vegetation Index (NDVI)

When sunlight strikes objects, certain wavelengths of this spectrum are absorbed and other wavelengths are reflected. A vegetation index is a spectral transformation of two or more bands used to compare different satellite images in order to obtain information of land cover.

The most common vegetation index is the NDVI and it relies on the fact that plants, specifically chlorophyll, strongly absorbs light in the red part of the visible spectrum (0.6 to 0.7  $\mu\text{m}$ ) for use in photosynthesis, and reflects light in the near infrared part of the spectrum (from 0.7 to 1.1  $\mu\text{m}$ ), mainly due to physical properties. The general signature of a leaf is presented in Figure 2.1.

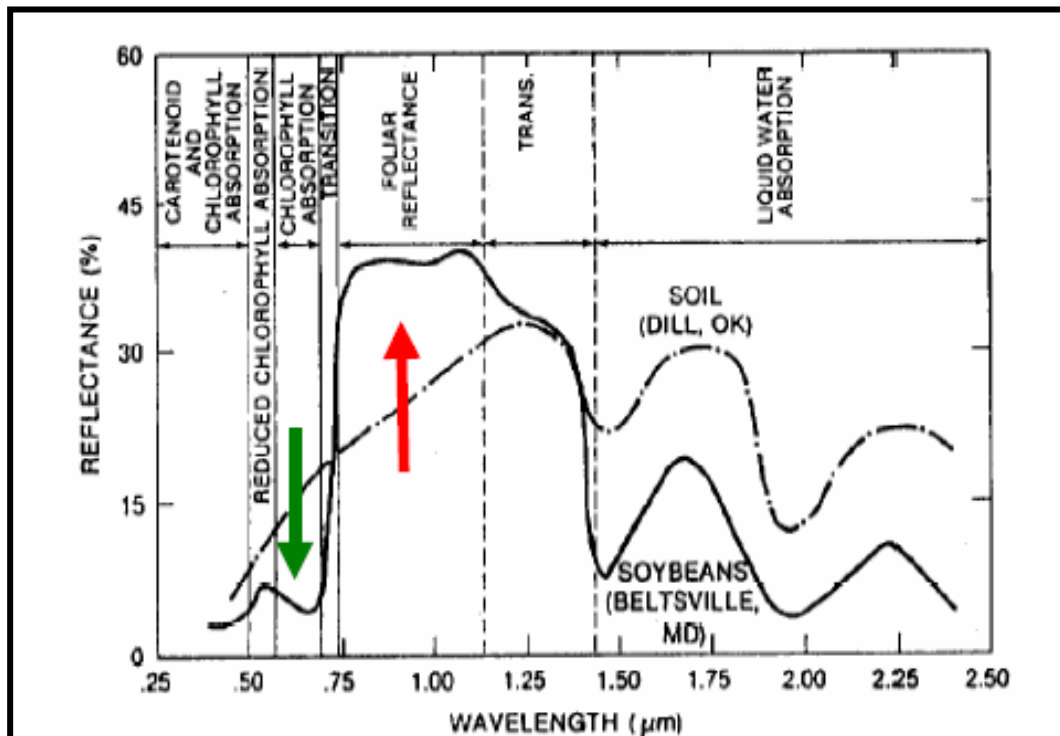


Figure 2-1 Typical Leaf Spectral Signature [6]

---

The difference between the reflection in the red part of the visible spectrum and the Near Infra Red (NIR) is used to determine a ratio called the NDVI, defined as:

$$NDVI = \frac{\rho_{NIR} - \rho_{red}}{\rho_{NIR} + \rho_{red}} \quad 2.1$$

As seen, it is normalized (rationed) to reduce the impact of aspects (noise) that are not related to surface cover, like atmospheric scattering and absorption, the soil background and variations of illumination; this is the strength of the NDVI.

The NDVI is successful as a vegetation measure in that it is sufficiently stable to permit meaningful comparisons of seasonal and inter-annual changes in vegetation growth and activity.

### *2.1.1 Satellite Spectrometers*

Many satellite instruments have been constructed for measuring NDVI, among them is MODIS (Moderate Resolution Imaging Spectral Radiometer). MODIS is a spectrometer that has 36 channels and is onboard Terra and Aqua satellites and has a spatial resolution that varies between 250m and 1000m. This satellite already has the bands defined for calculating NDVI, these are: bands 1 (0.62-0.67) and 2 (0.841-0.876) and have a resolution of 250m.

The NOAA Advanced Very High Resolution Radiometer (AVHRR) is another satellite that has been used for measuring NDVI. The AVHRR NDVI time series

---

(Pathfinder) has been successfully used in many studies on the interannual variability of global vegetation activity and in relating large-scale interannual variations in vegetation to climate. The bands used to calculate NDVI are bands 1 (0.58-0.68  $\mu\text{m}$ ) and 2 (0.72-1.0  $\mu\text{m}$ ) and they have a spatial resolution of 1Km. The AVHRR/3 instrument weighs approximately 72 pounds, measures 11.5 inches X 14.4 inches X 31.4 inches, and consumes 28.5 watts power. It was first carried on NOAA-15 and launched in May 1998.

The Landsat Thematic Mapper (TM) is another satellite used for measuring NDVI. Landsat TM bands that are used for calculating NDVI are bands 3 (0.63-0.69  $\mu\text{m}$ ) and 4 (0.76-0.90  $\mu\text{m}$ ). The TM was flown on Landsat-4 and Landsat-5 satellites. The TM is a cross-track scanner providing seven multispectral channels (3 visible, 1 near-infrared, 2 mid-infrared, 1 thermal-infrared) at 30-meter resolution (120-meter resolution for the thermal-infrared band). Landsat is a cornerstone of NASA's Earth Observing System (EOS).

### *2.1.2 Handheld Spectrometers*

Handheld spectrometers have been used to calculate NDVI, called narrow band indices, since the bands have a width of 10nm or less. The instrument is composed of a spectrometer, a personal computer, fiber optic cable, and different foreoptics for modification of the field of view. Inside the spectrometer instrument, light is projected from the fiber optics onto a holographic diffraction grating where wavelength components are separated and reflected for independent collection by the detectors [8]. A study was done in [8] and found that when using a handheld spectrometer with narrow bands the optimal results for NDVI were obtained by taking: the red band centered at

---

682nm with a bandwidth of 4nm and the NIR centered at 920nm and a bandwidth of 20nm.

## **2.2 Ground Penetrating Radar (GPR)**

The ground penetrating radar is a rapid, high-resolution tool for non-invasive investigation [9]. The radar waves propagate at velocities that are dependent upon the dielectric constant of the subsurface, and reflections are caused by sufficient changes in the dielectric constant that are due to changes in the subsurface medium. Interpretation of the reflected energy yields information on structural variation of the near subsurface.

### *2.2.1 Electromagnetic Background*

There are three fundamental measures of electromagnetic properties in materials: permeability, conductivity, and dielectric constant. These properties may influence the signal received by the GPR system and can provide information about the condition of the sub-surface. The electromagnetic properties depend on frequency; the dielectric constant of a material may not be the same at 1 MHz as it is at 1 GHz.

Permeability ( $\mu$ , henrys per meter) is the measure of the magnetic polarization of a material. Relative permeability of a material ( $\mu_r$ ) is the ratio of the permeability of a material to that of free space and is therefore dimensionless. Magnetic properties of most geological materials are the same as those of free space, and it is common to assume the relative magnetic permeability is equal to 1 [10].

---

Conductivity ( $\sigma$ , siemens per meter) is a measure of a material's ability to carry an electric current. Conductivity has a significant effect on the attenuation of a radar signal. The higher the conductivity the more will be the signal attenuation.

Permittivity ( $\epsilon$ , farads per meter) is a measure of the material's ability to resist formation of an electric field within it. Dielectric constant ( $\epsilon_r$ ) is the ratio of the permittivity of the material to that of free space and is therefore also called the relative permittivity and is dimensionless. The dielectric constant is primarily affected by moisture content. Figure 2.2 shows that for the same material, sand, the relative permittivity changes as the moisture changes [11].

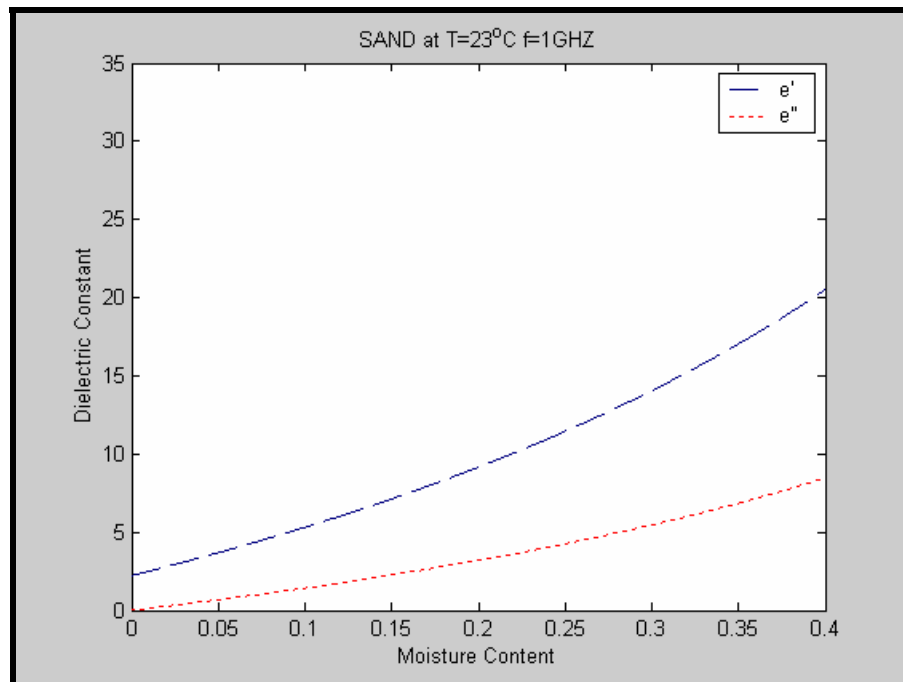


**Figure 2-2 Permittivity vs. Gravimetric Moisture**

### 2.2.2 Resolution

In the dictionary resolution is defined as the effect of an optical instrument in making the separate parts of an object distinguishable by the eye. Now more widely, the act,

---

process, or capability of rendering distinguishable the component parts of an object or closely adjacent optical or photographic images, or of separating measurements of similar magnitude of any quantity in space or time; also, the smallest quantity which is measurable by such a process. There different types of resolution: range resolution, spectral, spatial, radiometric, and temporal

Range resolution is the measure of how far apart two targets must be in order to be able to differentiate between the two (and not see both as a larger target) and is primarily determined by the wavelength, which is proportional to the pulse width [12]. Two objects are barely distinguishable from each other when they are separated by a wavelength. Closer than a wavelength, the objects appear as one, and farther than a wavelength they become more distinguishable from each other.

Wavelength ( $\lambda$ , meters) is the distance the waveform extends in space and is related to the frequency through the velocity of light in a particular material. The symbol used to represent wavelength is the Greek letter lambda ( $\lambda$ ) and the equation is shown below:

$$\lambda = \frac{c}{f} \quad 2-1$$

Another equation for wavelength can be derived in terms of the pulse width ( $\tau$ ):

$$\lambda = c\tau \quad 2-2$$

Two equal targets can be recognized as being resolved in range when they are separated a distance half this value, or  $c\tau/2$  [13].

Since the wavelength and frequency are inversely proportional, for higher frequency the wavelength is smaller resulting in higher resolution, and for lower frequencies the

---

wavelength is larger resulting in lower resolution. Thus, frequency has direct relationship with resolution and indirect relationship with the penetration range. The deepest penetration will occur in dry, non-clayey soils, and in dry rocks with no clay cementation. The strength of the echo is dependent on the absorption of the signal to and from the radar to the target, the size and shape of the target, and the degree of discontinuity at the reflecting boundary [14].

The spatial resolution of a sensor is perhaps the most intuitive or obvious characteristic of an image. The spatial resolution may be defined as a measure of smallest angular or linear separation between two objects that can be resolved by sensor. It is determined in large part by Instantaneous Field of View (IFOV). The IFOV is angular cone of visibility of the sensor (A, Fig 2.3) measured in radians and it determines the area seen from a given altitude at a given time (B). The area viewed is determined by  $\text{IFOV} * \text{altitude}$  (C). This calculation is known as ground resolution cell (GRC) or element (GRE)

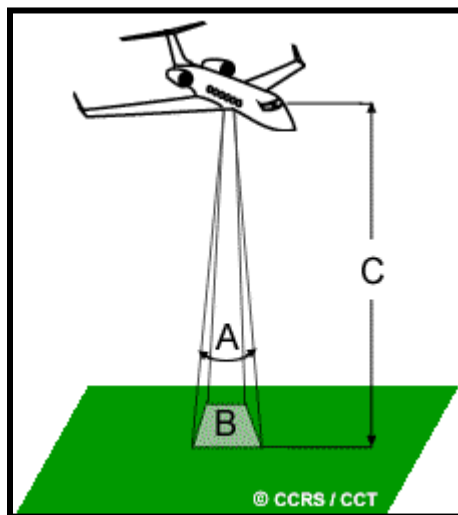


**Figure 2-3 Instantaneous Field of View (IFOV)**

---

The IFOV is a combination of geometric, mechanical and electronic properties of the imaging system. Geometric properties including satellite orbital altitude, detector size, and the focal length of the optical system; the sensitivity of each detector element at the wavelength desired plus the signal-to-noise level desired are electronic properties that determine a minimum time for energy absorption. Usually, each detector element in the array corresponds to a pixel in the image. Thus for a given altitude, the width of the pixel is determined by the optics and sensor size, and the height of the pixel is determined by the rate of forward motion. When magnified by the ratio of the sensor altitude to the focal length of the optics of the sensor system, IFOV is the size of the area on the ground represented by an individual detector element.

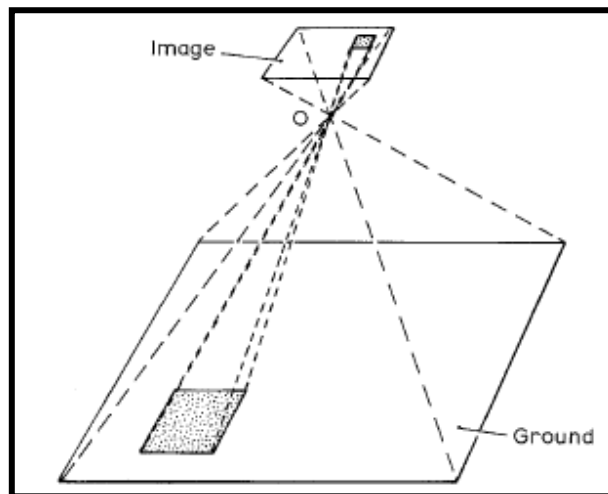


**Figure 2-4 Illustration of the geometrical instantaneous field-of-view reconstructed by projection from a pixel in the image plane.**

A sensor's spectral resolution is defined as the full-width-half-maximum (FWHM) of the instrument response to a monochromatic source.

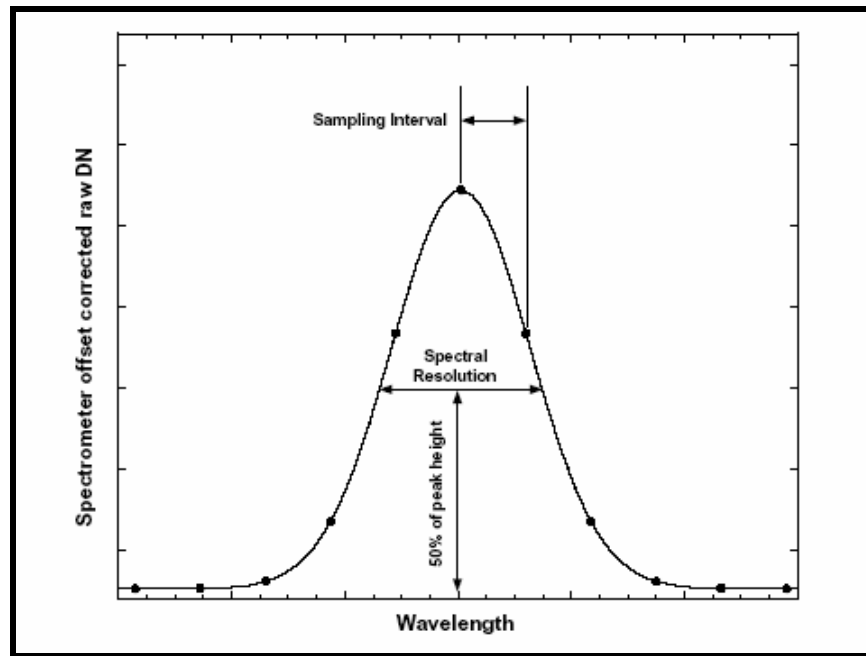


**Figure 2-5 Spectral Resolution**

Radiometric resolution refers to the number of possible values in each band of data. A high radiometric resolution allows finer distinction between values. The time between successive passes over the same region defines temporal resolution.

### 2.2.3 GPR Antennas

Electromagnetic energy is radiated and received by antennas. In a GPR system, it is necessary to have a transmitting and a receiving antenna. However, it is possible for a single antenna to simultaneously transmit and receive electromagnetic energy. Systems such as this are mono-static. Bi-static systems have separate transmitting and receiving antennas. An antenna is chosen based on desired resolution and penetration depth.

GPR antennas are either ground-coupled or air-coupled systems. Ground-coupled antennas operate at the surface resulting in deeper penetration. These systems are often

---

used to map bedrock and soil layers, and to detect pipes, buried drums and sub-surface contamination, but at slower collection rates than with the air-coupled systems. Typical center frequencies of ground-coupled antennas are between 50 MHz and 2.5 GHz.

Air-coupled antennas operate above the ground surface. Signals produced using air-coupled antennas include a recording of the transmitted signal as it travels through the air, called the direct coupling signal, visible as the first response. Typical center frequencies of air-coupled antennas are between 1 GHz and 2.5 GHz. Figures 2.6 and 2.7 are a general plot of one scan line (representative of time, and therefore depth) versus amplitude of the received signal.

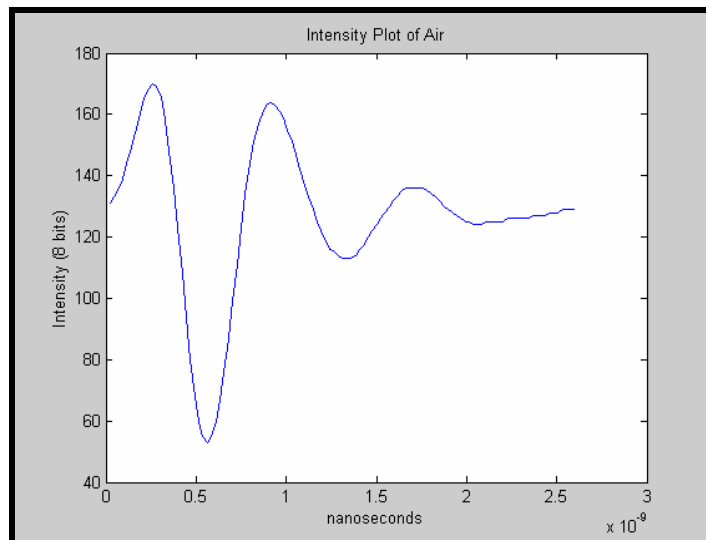


**Figure 2-6 Plot of sample scan line in air**

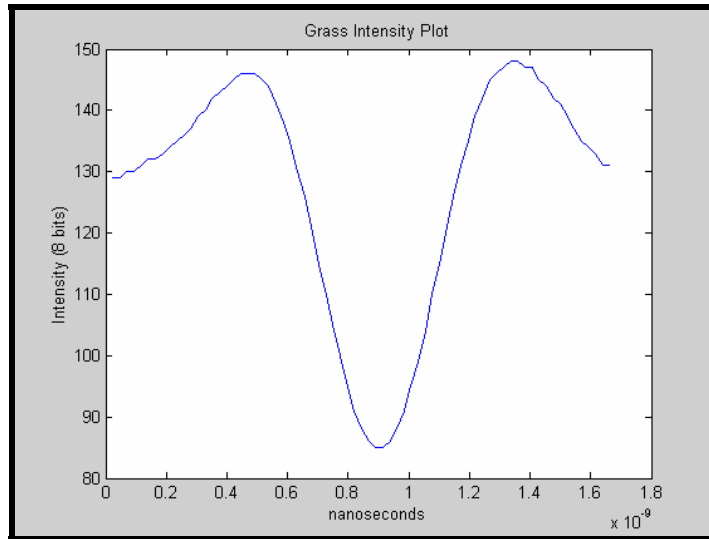


**Figure 2-7 Plot of sample scan line on top of a leaf**

#### *2.2.4 GPR Data Collection Terminology*

A trace or vertical scan is the record of the signal received by the receiving antenna (Figure 2.6). A trace is commonly shown as a plot of amplitude versus time of the reflected energy recorded by the receiving antenna. A trace is discretized in time and amplitude and a sample is each data point along the trace. Therefore, each sample has an associated two-way travel time and amplitude. The number of samples per scan indicates the number of data points in each scan. The data collection rate is the number of scans collected in a particular time or over a particular distance.

The process of collecting GPR data in the field typically begins with the collection of data files used in calibration and data processing. These files may include an air file providing information about the direct coupling signal and a metal plate shot providing a perfectly reflected signal. Data collected is digitized by a portable computer and stored for processing.

---

One of the benefits of GPR surveys is the ability to review the data on-site for quality control. To this end, filters may be used in the field to remove noise. This may be done using high and/or low pass filters to help filter out noise (frequencies much higher or lower than are of interest) prior to recording of data. Noise can also be removed from the raw data after survey completion.

## 2.3 Equipment and Materials

### 2.3.1 *Ground Penetrating Radar (GPR)*

The GPR used for this project is the GSSI SIR-20 manufactured by Geophysical Survey Systems, Inc, shown in Figure 2.8.



**Figure 2-8 The GSSI SIR-20**

It has two channels of data, transmit and receive, if using one antenna and four channels of data if using two antennas at the same time and it is a high performance GPR system. It is used to record, process, and display profiles and 3D images of subsurface features. The GPR has three methods of data collection: point mode, survey wheel, and free run mode. Point mode is collecting data one point at a time with a static antenna; the person decides how many scans they want by clicking on the mouse as many times as wanted. If the movement of the antenna is desired either the survey wheel or the free run

---

mode should be used, from these two the survey wheel is more precise. The survey wheel is calibrated and it records how many scan are obtained for 10 meters and the images can be used to accurately measure distance. The free run mode scans are obtained once you click the play button and stop when you click on the stop button; but the movements are not as consistent as with the survey wheel and measurements should not be used to measure distance, but may be used to observe a general view of the ground. For this experiment the point mode is chosen because the antenna is not moving is on top of the vegetation.

### 2.3.1.1 GPR Antenna

The frequency of operation is determined by the antenna chosen, the one used is the Model 5100 offered by GSSI company. It is a broadband antenna with range from 300MHz to 3GHz and center frequency of 1.5GHz, the depth range is from 0-.5 m (0-18 in), and dimensions are: 3.8 x 10 x 16.5 cm (1.5 x 4 x 6.5 in) and weight is 1.8 kg (4 lbs). It has two bow-tie antennas, separated by 60mm from each other, one is used for transmitting and the other one is used for receiving. The flare angle is 60°. Following there's a representation of the antennas inside the housing used.

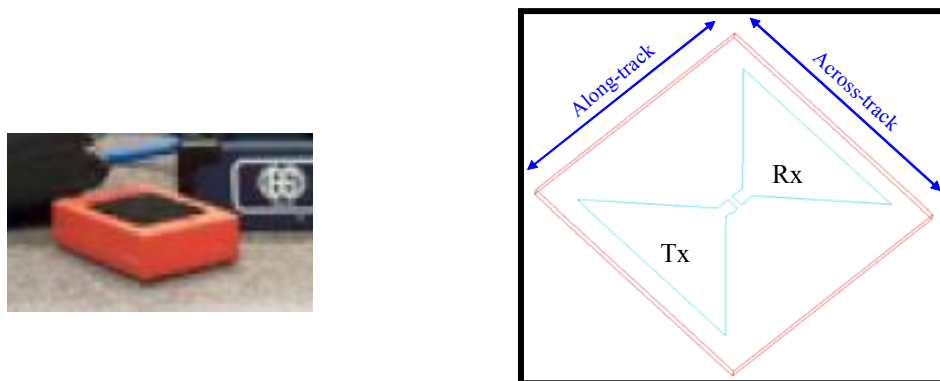


**Figure 2-9 The antenna (with housing) and its representation**

---

In order to determine the limitations of the antenna; how deep and how far apart it can receive what is backscattered, metal rods were placed at different depths; from 2” to 10”. The measurements with the GPR were taken using the survey wheel in order to take even measurements; this is why the images obtained have a parabola. The parabola is formed because as the GPR is moved it is sending and receiving a signal as it gets closer to the target the response is received faster, then as the GPR continues to move the signal delays more again. Figure 2.10 demonstrates how the intensity and the shape of the parabola, or reflected signal changes with different heights and the orientation of the antenna, along-track and across-track. From the images we can see that each image may be divided in three parts: the first lines, white, black, white is the interface ground-air, the second part, where the parabola is, is the reflections from the target. In order to be consistent the points taken were always on the white part of the parabola for the TE (along-track) mode and on the black part of the parabola for the TM (across track) mode. It can easily be seen that the intensity of the images obtained from the TM modes is much less than the intensity obtained from the TE modes.

Nine points were taken: the maximum, the tail of the parabola at the right, the tail of the parabola at the left, three points from the right end to the maximum and three points from the maximum to the left end. From these points we obtained the distance in the x axis in inches, the amplitude and the scan number.

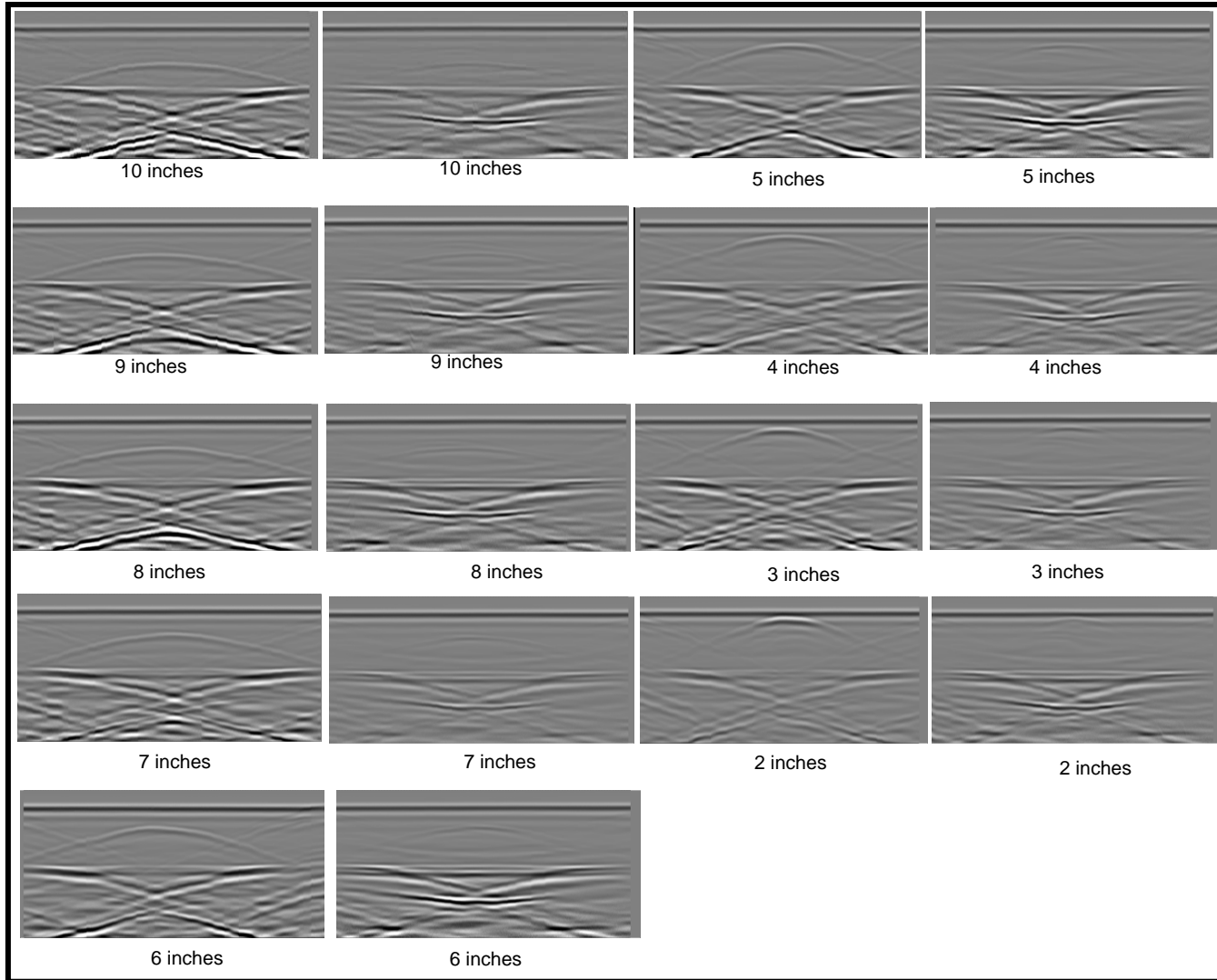


**Figure 2-10 GPR images taken both across and along track the antenna with a metal rod placed at different depths**

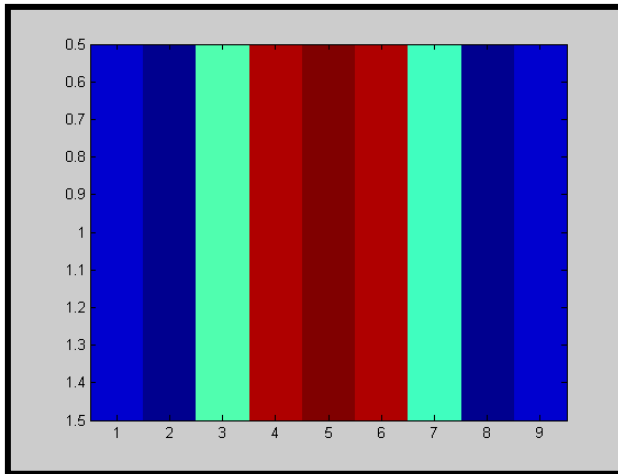


**Figure 2-11 The intensity distribution at the depth of two inches for TE mode**

Figure 2.11 images the 9 points taken at the depth of two inches. We can see that point 5 has the highest intensity, amplitude, and corresponds to the peak of the parabola and therefore the correct location of the rod. The ends of the parabola are represented by the blue. It may be noted that it appears symmetric and that points two and eight has lower amplitude than one and nine. This is due to the form of the radiation pattern.

**TABLE 2-1 TM Data**

TM	
Depth (in)	Parabola's width (in) from end to end
2	2.23
3	7.07
4	4.5
5	10.3
6	12.5
7	5.33
8	10.59
9	12
10	9.13

**TABLE 2-2 TE Data**

TE	
Depth (in)	Parabola's width (in) from end to end
2	10.6
3	9.43
4	12.73
5	25.5
6	26.4
7	25.53
8	25.5
9	23.8
10	23.17

The values shown in Table 2.1 and 2.2 were used to obtain the 3-D Radiation Pattern using Matlab®. Plotting the values obtained results in a radiation pattern of the antenna shown in figure 2.12. Once again it shows that in TE, or along-track, the intensity is higher and the pattern is wider (observe the scale) and more uniform.

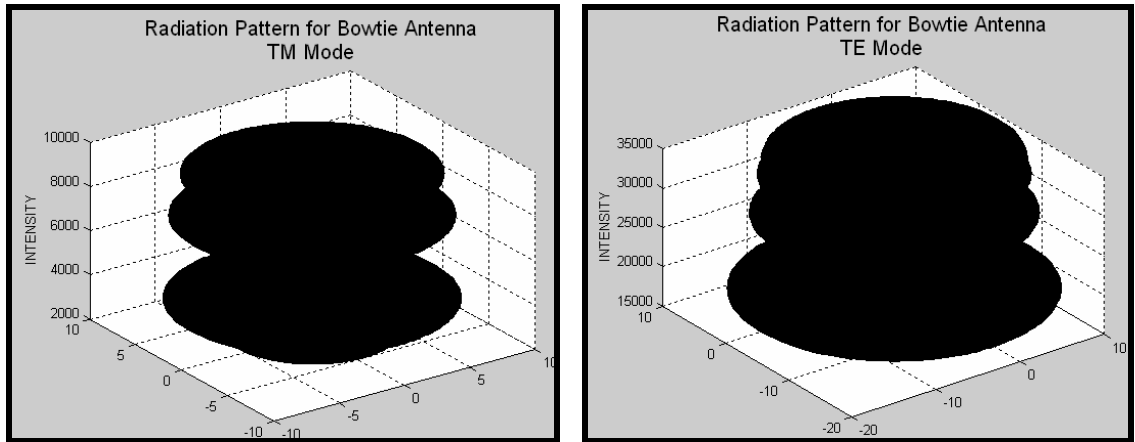


**Figure 2-12 Radiation Pattern Across and Along Track**

### 2.3.2 Spectral Radiometer

The Spectrometer used is the FieldSpec Handheld Spectrometer manufactured by Analytical Spectral Devices, Inc, shown in Figure 2.13.



**Figure 2-13 The FieldSpec Handheld Spectrometer**

It has a spectral range of 325-1075 nm. The spectral resolution is 3.5 nm @ 700 nm and it has a sampling interval of 1.6 nm @ 325-1075 nm.

### 2.3.3 Software Used

The software used to analyze the data obtained from the GPR is:

- RADAN, program provided by the GSSI company.

- 
- Matlab®, program that will be used to process the data to obtain frequency and phase spectrums and also calculate the average power of the signal obtained from the GPR.
  - Microsoft Office Excel

#### 2.3.4 *Plantain Leaves*

The experiments were done using plantain leaves in different states of health, from very dry (brown), categorized as level 1, to very moist (green), categorized as level 6.



**Figure 2-14 Vegetation Levels**

---

## 3 EXPERIMENT SETUP AND METHODOLOGY

### 3.1 Data Acquisition

Plantain leaves were cut from banana trees during different days in order to have a varied set of vegetation health. The leaves were separated into six categories and labeled according to their health; being 1 the driest and 6 the healthiest. These leaves were then first put under the spectrometer and then under the GPR. This was done twice in order to have an even more varied set.

The first part of this experiment is the calibration of the instrument using a white reference. The experiment was done during the day and outdoors because the spectrometer needs the light in order to measure the reflectance from the sun. One leaf of each level was placed under the spectrometer, as shown in figure 3.1.



**Figure 3-1 Spectrometer Experiment Setup**

From a series of spectrums the system averages them in order to eliminate any error from movement or background. The spectrums for each level have a spectral range of 325-1075 nm, the one the instrument offers. Afterwards the GPR was placed above a pack of leaves of the same level and the data is collected using point mode (0 feet) from the leaves. A data log was created.

---

## 3.2 Data Analysis

From the data obtained by the spectrometer, NDVI was calculated using formula 2.1. The specific values of wavelength used were the ones explained in section 2.1.2; the red band centered at 682nm with a bandwidth of 4nm and the NIR centered at 920nm and a bandwidth of 20nm. The values from the red band were first averaged and so was NIR band. Using the average values of the red and NIR bands, formula 2.1 was used to calculate NDVI value.

The data obtained from the GPR was first corrected. For this process a scan line was chosen and introduced in Matlab®, Figure 3.4. Fourier transform was done on the scan line data, changing the data from the time domain to the frequency domain, in order to obtain the amplitude and the phase spectrum of the scan.

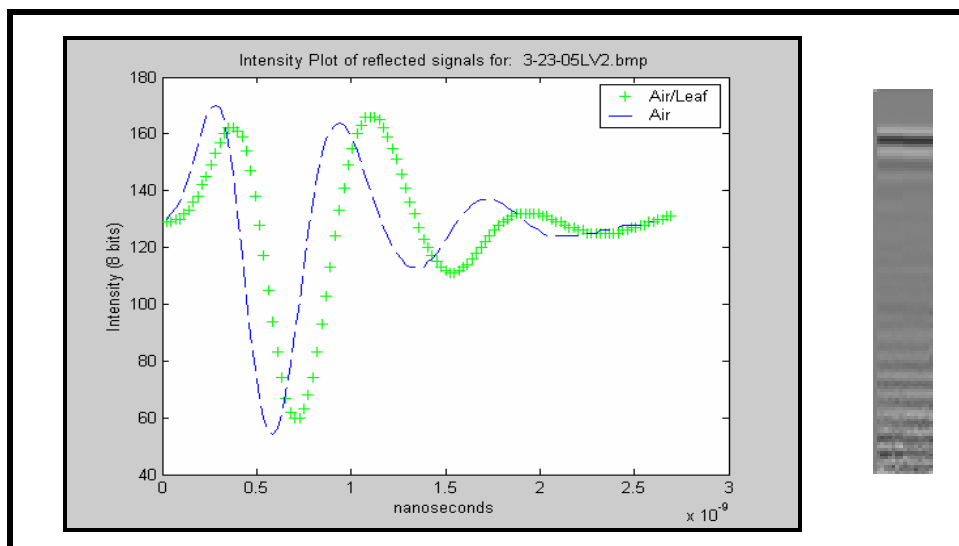


**Figure 3-2 Image obtained from GPR for leaf level #2 and the intensity of a scan line of vegetation and air represented in Matlab ®**

---

This was done to the backscattered signal of air alone and to the backscattered signal of air/leaf. Two methods of signal subtraction and deconvolution were studied to separate the air signal reflection from the vegetation signal reflection. The usefulness of each one was analyzed.

The first try was signal subtraction, where a constant direct coupling was assumed and this signal would be subtracted from the signal reflected from the leaf. Studying this it was noticed that the process that occurred was convolution and not addition so this method was discarded.

The images obtained from the GPR are a convolution of the original signal and the material characteristics [15]. We can look at this problem from a systems perspective, where:

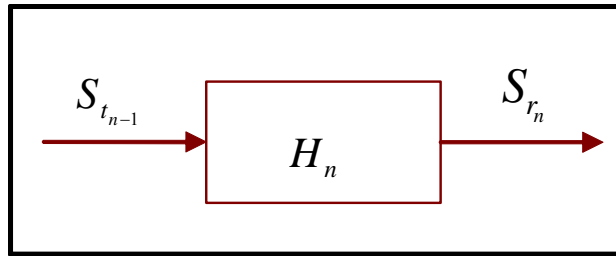
$$S_{r_n}(t) = S_{t_{n-1}}(t) * H_n(t) \quad 3-1$$

or similarly as,

$$S_{r_n}(f) = S_{t_{n-1}}(f) \cdot H_n(f) \quad 3-2$$

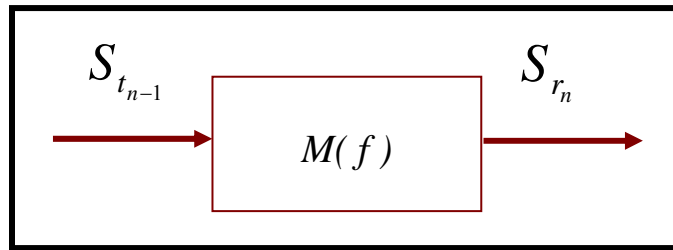
since convolution in the time domain is a multiplication in the frequency domain.

Figure 3.3 depicts the systems representation of the soil type characteristics, the transmitted wave into that layer and the reflected wave.



**Figure 3-3 System Representation of the layer characteristics, the transmitted and reflected waves.**

Because this is a convolution operation,  $S_{r_n}$  has to be longer than  $S_{t_{n-1}}$  but this is not the case for soil but it is the case for vegetation. Material Characteristics in Fourier Domain (MCFD) is the  $H_n$  of the system where the transmitted signal is modified by the MCFD producing  $S_{r_n}$  where  $n$  is one (1) because there is only one layer. Figure 3.4 shows the system where  $M_n$  is the defined MCFD.



**Figure 3-4 System Representation for the new layer characteristics, the transmitted and reflected waves.**

From figure 3-4 it is possible to see that

$$S_{r_1}(f) = M_1(f) \cdot S_{t_0}(f) \quad 3-3$$

consequently we obtain equation 3.4, which is in discrete Fourier notation.

$$M_1(f) = \frac{S_{r_1}(f)}{S_{t_0}(f)} \quad 3-4$$

Then using the amplitudes of the corrected spectrum the average power was calculated using equations 3.5.

$$P_{ave} = \frac{\sum_{i=1}^N A(f_i)^2}{N} \quad 3-5$$

Where A is the amplitude of the MCFD at different frequencies, and N is the number of frequencies chosen.

This process was implemented using Matlab ®, a flowchart of the code is presented in Figure 3.5.

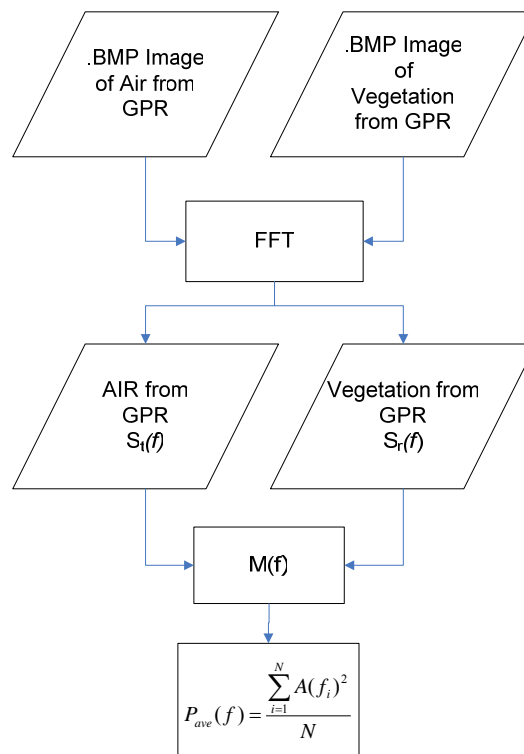


**Figure 3-5 Flowchart for Matlab Program**

These results were plotted against the results obtained from the NDVI calculation and a relationship was found between them. The results appear in the subsequent chapter.

---

## 4 ACTIVE VEGETATION INDEX VS. NDVI

The analysis and determination of the Active Vegetation Index and its relationship to the NDVI is presented. All of the data collected is shown and how it was used. Data was collected in three times, only the last two are presented. The first set of data had a piece of wood as background and for this reason it was not chosen to be analyzed further. The second and third set of data had only air as background, these were the ones chosen. The Spectrometer Experiment and its results are shown first, then the GPR Experiment and finally the correlation.

### 4.1 First Set

This set of data was taken on March 23, 2004

#### 4.1.1 *Spectrometer Experiment*

One spectrum of each level is plotted in Figure 4.1 starting only at 500nm so that the detail of the signature could be seen better and also, the wavelengths below 500nm are not needed.

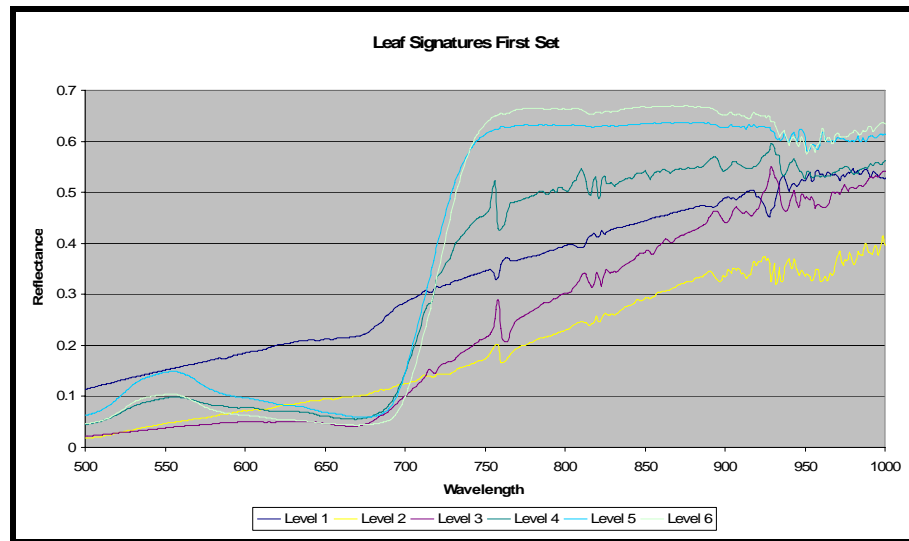


**Figure 4-1 Spectrums of each level of health of the plantain leaves**

It may be seen that all signatures have similar shapes, since the shape depends on the structure of the leaf and all leafs are the same type. As it gets dryer the shape gets worst.

Using the average values of the red and NIR bands, equation 2.1 is used to calculate the NDVI. The results are shown in Table 4.1.

**TABLE 4-1 NDVI for each level**

Leaf Level	NDVI
1(Dry)	0.3165
2	0.4343
3	0.7908
4	0.819
5	0.852
6 (Green)	0.86

---

### 4.1.2 GPR Experiment

For each leaf level the intensity plot for the air signal and the leaf reflection is represented in Matlab and the MCFD is calculated afterwards, it is shown in figures 4.2 through 4.13. The amplitudes to enter in equation 3.5 are obtained from the data from the MCFD signatures and the results are shown in Table 4-2.

#### 4.1.2.1 Leaf Level #1

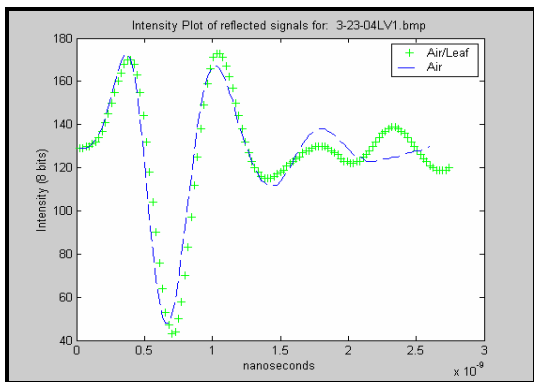


**Figure 4-2 Intensity Plot for Leaf Level #1**

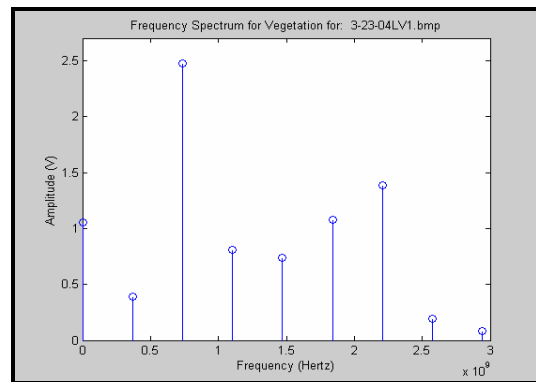


**Figure 4-3 MCFD for Leaf Level #1**

The average power for this level is 0.2349W.

#### 4.1.2.2 Leaf Level #2

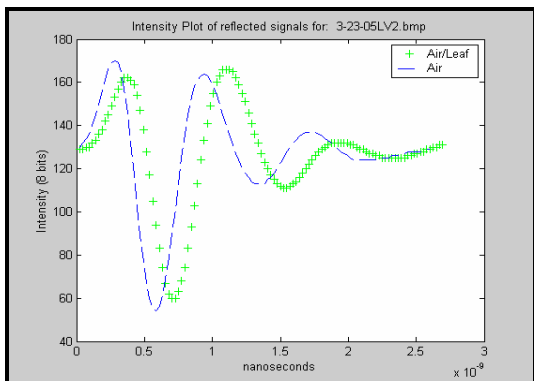


**Figure 4-4 Intensity Plot for Leaf Level #2**

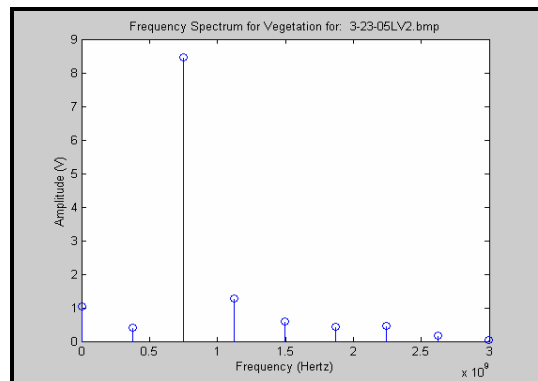


**Figure 4-5 MCFD for Leaf Level #2**

The average power for this level is 0.2066W.

### 4.1.2.3 Leaf Level #3

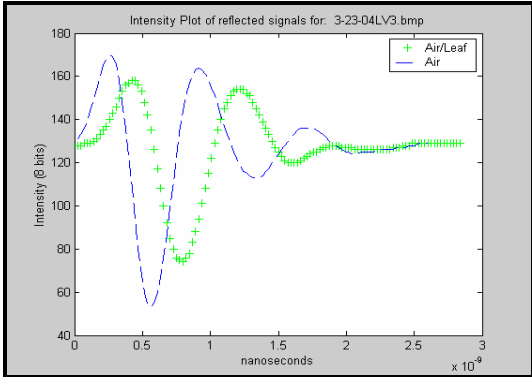


**Figure 4-6 Intensity Plot for Leaf Level #3**

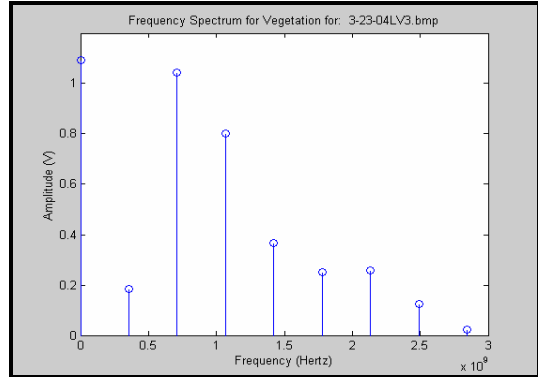


**Figure 4-7 MCFD for Leaf Level #3**

The average power for this level is 0.3789W.

### 4.1.2.4 Leaf Level #4

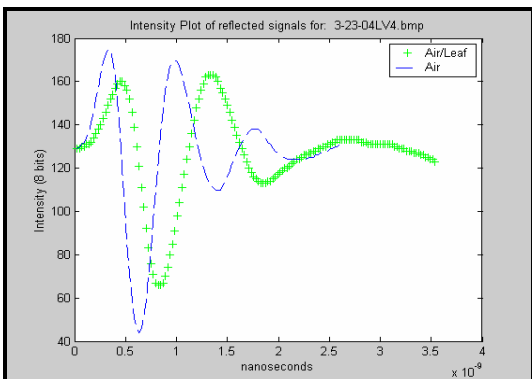


**Figure 4-8 Intensity Plot for Leaf Level #4**

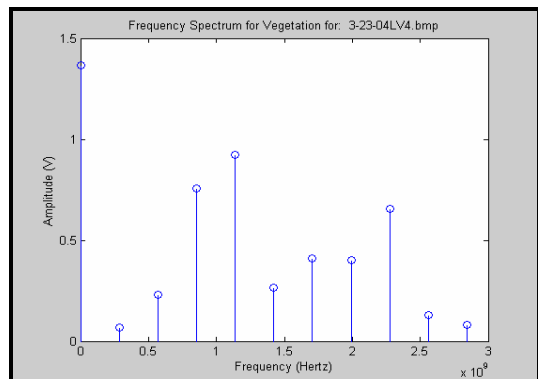


**Figure 4-9 MCFD for Leaf Level #4**

The average power for this level is 0.0976W

#### 4.1.2.5 Leaf Level #5.

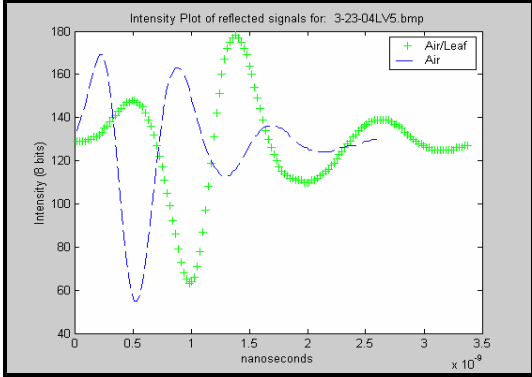


**Figure 4-10 Intensity Plot for Leaf Level #5**

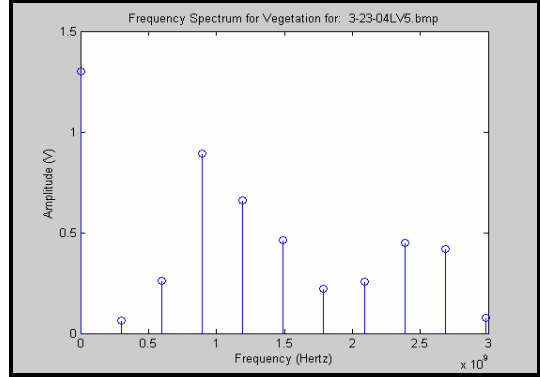


**Figure 4-11 MCFD for Leaf Level #5**

The average power for this level is 0.0745 W.

#### 4.1.2.6 Leaf Level #6

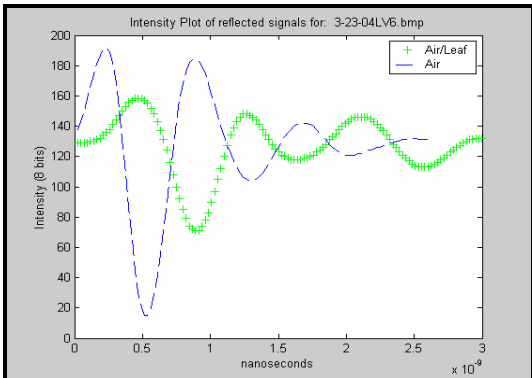


**Figure 4-12 Intensity Plot for Leaf Level #6**

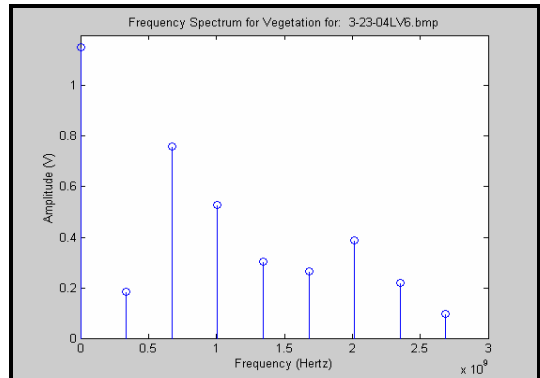


**Figure 4-13 MCFD for Leaf Level #6**

The average power for this level is 0.0926 W

---

#### 4.1.2.7 Average Power for All of the Levels

**TABLE 4-2 Average Power for All Levels**

Classification	Average Power (W)
1(Dry leaf)	0.02349
2	0.2066
3	0.3789
4	0.0976
5	0.0745
6 (Green leaf)	0.0926

## 4.2 Second Set

The second set of data was taken on April 14, 2004

### 4.2.1 Spectrometer Experiment

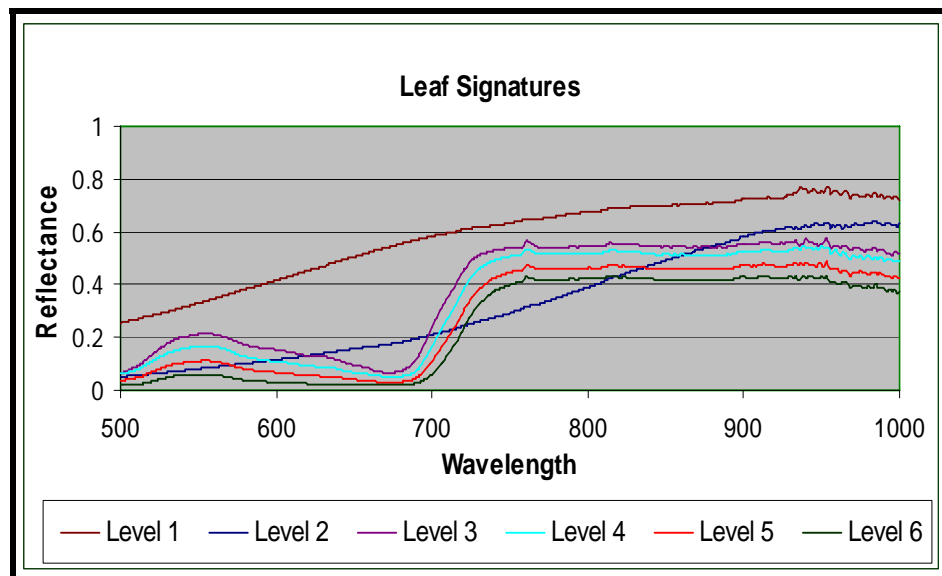


**Figure 4-14 Spectrums of each level of health of the banana leaves.**

Using the average values of the red and NIR bands, equation 2.1 will be used to calculate NDVI values. The results for the NDVI are shown in Table 4-3.

**TABLE 4-3 NDVI for each level**

Leaf Level	NDVI
1(Dry)	0.13
2	0.53
3	0.75
4	0.81
5	0.86
6(Green)	0.90

#### 4.2.2 GPR Experiment

The GPR experiment for this set was exactly the same as set #1. The results are shown in figures 4.15 through 4.26. The MCFD was used to calculate the average power and is shown in Table 4-4.

##### 4.2.2.1 Leaf Level #1

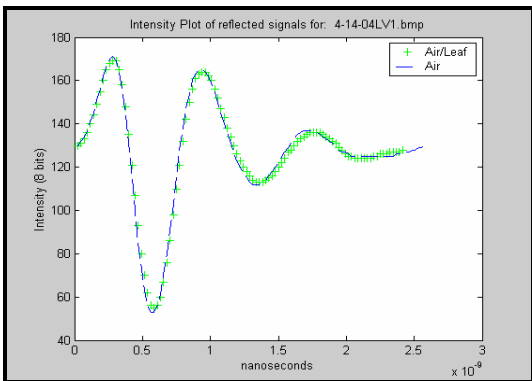


**Figure 4-15 Intensity Plot for Leaf Level #1**

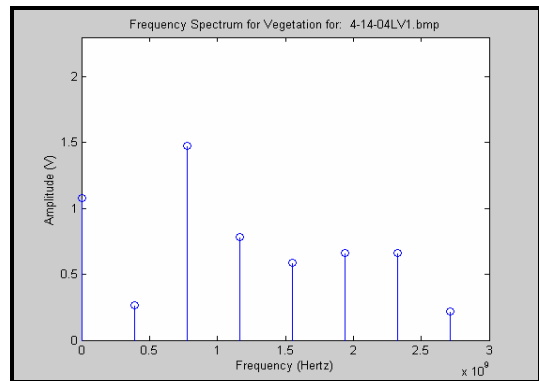


**Figure 4-16 MCFD for Leaf Level #1**

The average power for this level is 0.2021W.

### 4.2.2.2 Leaf Level #2

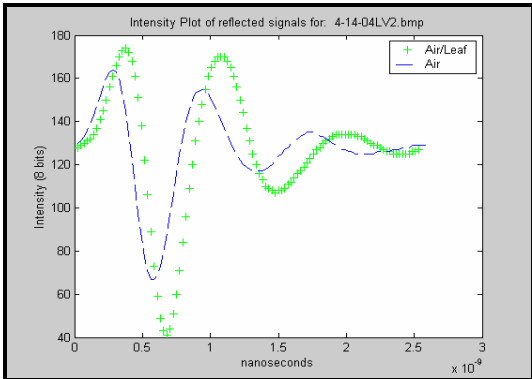


**Figure 4-17 Intensity Plot for Leaf Level #2**

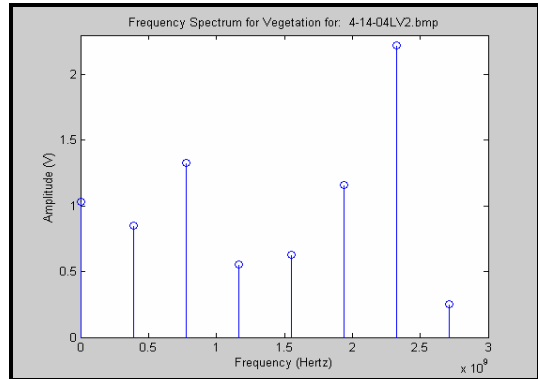


**Figure 4-18 MCFD for Leaf Level #2**

The average power for this level is 0.4796 W.

### 4.2.2.3 Leaf Level #3

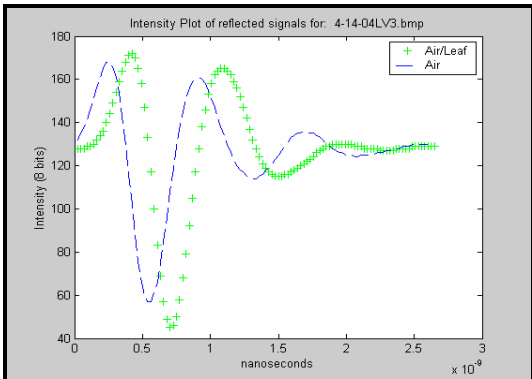


**Figure 4-19 Intensity Plot for Leaf Level #3**

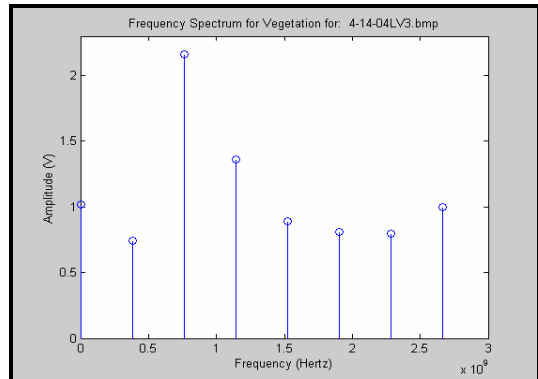


**Figure 4-20 MCFD for Leaf Level #3**

The average power for this level is 0.2665 W.

#### 4.2.2.4 Leaf Level #4

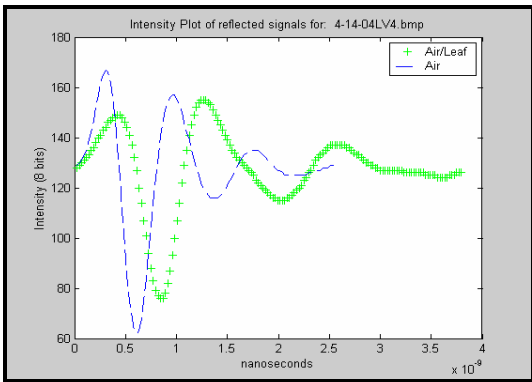


**Figure 4-21 Intensity Plot for Leaf Level #4**

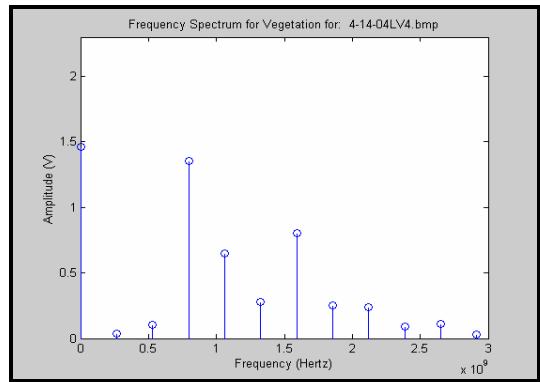


**Figure 4-22 MCFD for Leaf Level #4**

The average power for this level is 0.1508 W.

#### 4.2.2.5 Leaf Level #5

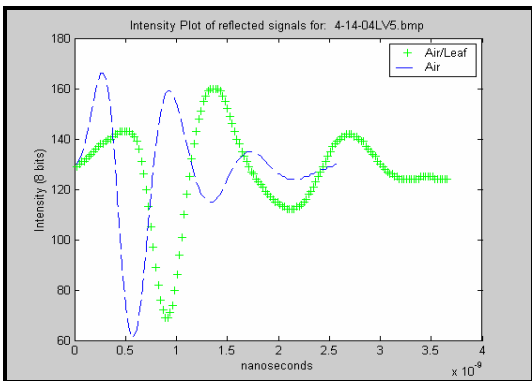


**Figure 4-23 Intensity Plot for Leaf Level #5**

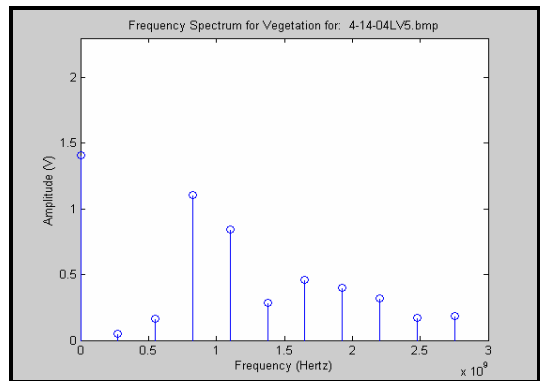


**Figure 4-24 MCFD for Leaf Level #5**

The average power for this level is 0.1019 W.

### 4.2.2.6 Leaf Level #6

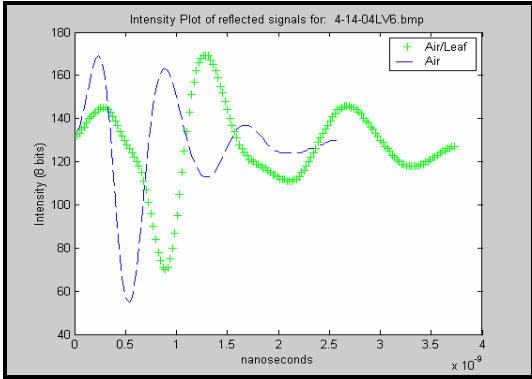


**Figure 4-25 Intensity Plot for Leaf Level #6**

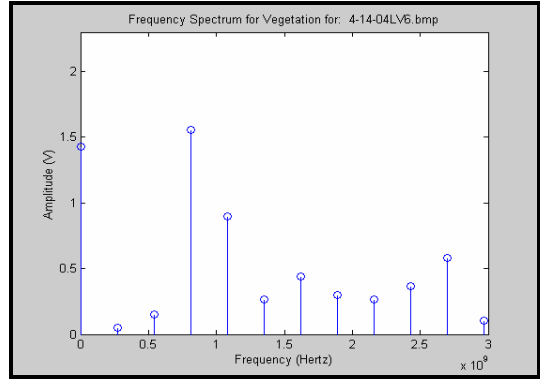


**Figure 4-26 MCFD for Leaf Level #6**

The average power for this level is 0.0797 W.

### 4.2.2.7 Average Power for All of the Levels

**TABLE 4-4 Average Power for All Levels**

Classification	Average Power (W)
1(Dry leaf)	0.2021
2	0.4796
3	0.2665
4	0.1508
5	0.1019
6 (Green leaf)	0.0797

---

### 4.3 Combined Results

The results of the two sets were combined. All the results for the NDVI, Tables 4.1 and 4.3, were plotted against the results obtained from the GPR, the average power from the MCFD; Tables 4.2 and 4.4. The data was entered in Excel © and was fitted linearly using least squares. The Pearson product moment correlation coefficient, R, defined in equation was used:

$$R = \frac{\sum (x - \bar{x})(y - \bar{y})}{\sqrt{\sum (x - \bar{x})^2 \sum (y - \bar{y})^2}} \quad 4-1$$

Where x is the set of data of the NDVI and y is the set of data of the MCFD power, and  $\bar{x}$  and  $\bar{y}$  are the averages. The plot of the data along with its linear fit equation is shown in Figure 4.27.

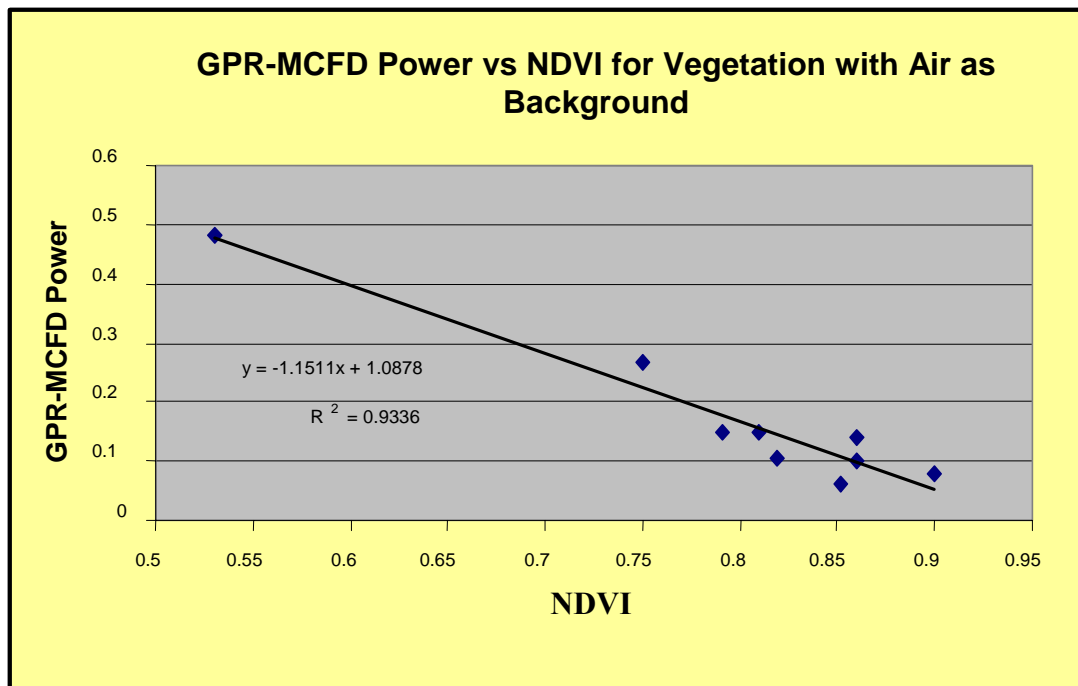


Figure 4-27 GPR-MCFD Power vs. NDVI

---

The correlation (R) obtained is -0.97, it is negative because it is an inverse relationship; as NDVI goes higher, MCFD power minimizes. The correlation coefficient R not showed in the plot, but  $R^2$ . The squared correlation coefficient ( $R^2$ ) is the proportion of variance in Y that can be accounted for by knowing X. Conversely, it is the proportion of variance in X that can be accounted for by knowing Y. It is also known as the coefficient of determination. In the experiment the coefficient of determination is 93.3%.

---

## 5 CONCLUSIONS AND FUTURE WORK

An inverse linear relationship was found between the power of the signal backscattered from the leaves and the NDVI, for NDVI greater than 0.5. We can see that it is an inverse relationship with a correlation of -0.97, which is close to 1, a perfect fit. There are jumps in the range of NDVI, and the results for NDVI less than 0.5 are left out because they need another methodology since its reflection is too close to the air's reflection.

It was known that radar signal gets attenuated with water because of its high conductivity. Water inside the vegetation is moisture, the healthier the vegetation the more water it retains, therefore it was expected that the higher the vegetation index the lower the signal backscattered [15]. This measurement was done with power of the signal in the frequency domain. The results obtained were as expected and a correlation was found.

For future research more measurements are needed in order to fill for the gaps of NDVI. The ultimate goal of the investigation is to obtain these measurements and results using remote instruments. Consequently, for future work observation of a vegetation canopy using SAR and Landsat TM is to be done, in order to validate the relationship between NDVI and MCFD Power, and finally define the new active vegetation index.

---

## REFERENCES

- [1] Inoue, Y., Kurosu, T., Maeno, H., Uratsuka, S., Kozu, T., Dabrowska-Zielinska, K., Qi, J., “Season-long daily measurements of multifrequency (Ka, Ku, X, C, and L) and full-polarization backscatter signatures over paddy rice field and their relationship with biological variables”, *Remote Sensing of Environment* 81 (2002) 194– 204.
- [2] Tuong Thuy, V. and Tokunaga, M., “Effect of Coherence on Dems Derived from SAR Interferometry: A Case Study of Mayon Volcano, Philippines,” *Mapping from Space and GPS, Asian Conference on Remote Sensing*, 2000.
- [3] Tokunaga, M., Tuong Thuy, V., “Finding the Relationship Between Vegetation Index And Coherence Signature To Utilize The Product Of Radar Interferometry In Land Cover Application”, *Asian Conference on Remote Sensing*, 2002.
- [4] Matsumoto, K., Sakai, T., Torii, S. “Relating JERS-1 Data to NDVI by Monitoring Various Forests,” *Asian Conference on Remote Sensing*, 2001.
- [5] Butnor, J. R., Doolittle, J. A, Kress, L., Cohen, S. and Johnsen, K. H., “Use of ground-penetrating radar to study tree roots in the southeastern United States”, *Tree Physiology* 21, 1269-1278. Heron Publishing - Victoria, Canada, 2001
- [6] Huete, A., “5. Optical Properties of Plant Canopies,” [http://tbrs.arizona.edu/education/553-2002/Ch5\\_Veg\\_lect.pdf](http://tbrs.arizona.edu/education/553-2002/Ch5_Veg_lect.pdf).
- [7] Weier, J. and Herring D., “Measuring Vegetation (NDVI & EVI)”, *Earth Observatory*, <http://earthobservatory.nasa.gov/Library/MeasuringVegetation>.
- [8] Thenkabail, P. S., Smith, R.B and De Pauw, E., “Hyperspectral Vegetation Indices and Their Relationships with Agricultural Crop Characteristics,” *Remote Sensing Environ.* 74:158-182, Elsevier Science Inc., 2000.
- [9] Cardimona, S., Webb, D.J. and Lippincott, T., “Ground Penetrating Radar,” *Geophysics* 2000.
- [10] Sadiku, M. “Elements of Electromagnetics”, *Harcourt Brace college Publishers*, Philadelphia 1989.
- [11] Torres, M., Parsiani, H. “Non-linearity of Soil Dielectric as a Function of Radar Frequency and Soil Moisture Content”. *A peer review, Proc. CRC'2004*, April 2, 2004, Mayaguez, P.R.

- 
- [12] Kingsley and Quegan, "Understanding Radar Systems". Mc Graw Hill, London, 1992.
- [13] Skolnik, M. I, "Introduction to Radar Systems", McGraw Hill Higher Education, 3<sup>rd</sup> Ed, 2001.
- [14] Dolphin, L., "A Brief Background On Ground Penetrating Radars," <http://www.ldolphin.org/>, 1997.
- [15] Parsiani, H., Torres, M., Rodriguez, P., "Material Characteristics In Fourier Domain (MCFD) Formulation, A Signature To Determine Soil Type, Moisture, And Vegetation Health, Based On Multilayer Ground Penetrating Radar Reflection." *SIP 2004*, Hawaii.
- [16] Le Vine, D. M., "Dependence of Attenuation in a Vegetation Canopy on Frequency and Plant Water Content", IEEE Transactions on Geoscience and Remote Sensing, VOL. 34, NO.4, September 1996
- [17] Redman, Galagedara, and Parkin, "Measuring Soil Water Content with the Ground Penetrating Radar Surface Reflectivity Method: Effects of Spatial Variability" 2003 ASAE Annual International Meeting, ASAE 2003
- [18] Parsiani, H., Torres, M., Rodriguez, P., "High Resolution Vegetation Index as Measured by Radar and its Validation with Spectrometer", SPIE 2004, Sept. 2004, Spain

---

## APPENDIX A

## MATLAB CODE FOR MCFD

```
%Program for MCFD in the first layer
clear all
close all
clc
[filename pathname]= uigetfile (*.bmp', 'Please select your image to calculate media');
truefile =[pathname filename];
[X1 , map]= imread (truefile);    %reading the input picture

[filename2 pathname2]= uigetfile (*.bmp', 'Please select your image for air'); %User select image for air
truefile2=[pathname2 filename2];
[X2 , map]=imread (truefile);    %reading the input picture for air

fs =512/(12*1.0e-009); %Sampling Frequency%
display=(2:10); % To eliminate DC from plotting

scannum1=input ('Please enter the scan number desired for the vegetation: ');
%Enter the scan number obtained from the data log for Air/Leaf

samples1=input ('Please enter the samples in the form (#:#) ');
%User enters the samples to be used

scan1 (:,1)= double(X1(samples1,scannum1));

imshow (X1,map,'notruesize');title(['GPR image file ', num2str(filename)]);
%drawing the input images

scannum2= input('Please enter the scan number desired for air: ');
samples2=input('Please enter the samples in the form (#:#) ');
scan2(:,1)= double(X2(samples2,scannum2));

t1=(1:length(scan1))/fs;
t1=t1';

t2=(1:length(scan2))/fs;
t2=t2';

figure;
plot(t1,scan1,'+g',t2,scan2,'--b');
legend('Air/Leaf', 'Air');
title(['Intensity Plot of reflected signals for: ', num2str(filename)]);
xlabel ('nanoseconds');
ylabel ('Intensity (8 bits)');

freq1=fft (scan1);
freq2=fft (scan2);

mag1=abs (freq1);
mag2=abs (freq2);

figure;
```

---

```

f1 = ((display-1)*fs/length(t1));
f2 = ((display-1)*fs/length(t2));

if (length(scan1)<=length(scan2)); %Inverse Characteristics
    V= fft ([scan1' zeros (1,length(scan2)-length(scan1))]);
    Z=fft (scan2');
    x=double (scan1);
    y=double (scan2);
    largomedia = length(scan2)-length(scan1)+1;
%Forward Characteristics
else
    V= fft([scan2' zeros(1,length(scan1)-length(scan2))]);
    Z=fft(scan1');
    x=double(scan2);
    y=double(scan1);
    largomedia=length(scan1)-length(scan2)+1;
    %display('Inverse characteristic of Soil');
end
media=Z./V;
inverse_fourier=ifft(media);
inverse_fourier_media=inverse_fourier(1:largomedia);

N = length(media);
f = [0:N-1]*fs/(N-1);

mag=abs(media);
figure;
stem(f,mag);
axis([0 3000000000 0 2.3]);
xlabel ('Frequency (Hertz)');
ylabel ('Amplitude (V)');
title(['Frequency Spectrum for Vegetation for: ', num2str(filename)]);

display=(2:length(mag)); %Use this one to calculate the power for the whole spectrum

AvgPower = avg(mag(display).^2, 12) %Average Power of the first 12 data of the MCFD
AvgPowerall = avg(mag.^2,116) %Average power of all the data of the MCFD
DCPower = mag(1)^2 %Average power of the first data, DC

```

---

## APPENDIX B DATA FROM SPECTROMETER

### B.1 First Set of Data, 3-22-2004

NDVI LEVEL 6				
VISIBLE RED		NIR		NDVI
$\lambda(\text{nm})$	Reflectance	$\lambda(\text{nm})$	Reflectance	
650	0.042	900	0.478	0.839
651	0.041	901	0.476	0.840
652	0.041	902	0.473	0.841
653	0.040	903	0.473	0.844
654	0.040	904	0.475	0.846
655	0.039	905	0.475	0.848
656	0.038	906	0.477	0.852
657	0.037	907	0.480	0.856
658	0.037	908	0.482	0.857
659	0.037	909	0.481	0.858
660	0.036	910	0.478	0.859
661	0.036	911	0.478	0.862
662	0.035	912	0.479	0.864
663	0.034	913	0.481	0.867
664	0.034	914	0.481	0.867
665	0.034	915	0.480	0.868
666	0.034	916	0.479	0.869
667	0.033	917	0.479	0.871
668	0.033	918	0.481	0.873
669	0.033	919	0.473	0.871
670	0.032	920	0.467	0.870
671	0.032	921	0.465	0.871
672	0.032	922	0.468	0.872
673	0.032	923	0.471	0.873
674	0.032	924	0.470	0.872
675	0.032	925	0.468	0.871
676	0.032	926	0.465	0.870
677	0.033	927	0.469	0.870
678	0.033	928	0.477	0.872
679	0.033	929	0.493	0.875
680	0.034	930	0.502	0.873
681	0.035	931	0.510	0.873
682	0.035	932	0.516	0.872
683	0.037	933	0.510	0.866
684	0.038	934	0.496	0.858
685	0.040	935	0.479	0.848
			Avgndvi	0.863
			OptNDVI	0.859

---

NDVI LEVEL 5				
VISIBLE RED		NIR		NDVI
$\lambda(\text{nm})$	Reflectance	$\lambda(\text{nm})$	Reflectance	
650	0.051	900	0.637	0.852
651	0.051	901	0.638	0.853
652	0.050	902	0.635	0.854
653	0.050	903	0.633	0.855
654	0.049	904	0.630	0.855
655	0.049	905	0.630	0.855
656	0.049	906	0.632	0.857
657	0.048	907	0.635	0.859
658	0.049	908	0.636	0.858
659	0.049	909	0.636	0.858
660	0.048	910	0.635	0.860
661	0.048	911	0.633	0.859
662	0.048	912	0.632	0.860
663	0.047	913	0.632	0.860
664	0.047	914	0.633	0.860
665	0.048	915	0.633	0.860
666	0.048	916	0.632	0.860
667	0.047	917	0.634	0.861
668	0.047	918	0.637	0.862
669	0.047	919	0.635	0.861
670	0.047	920	0.633	0.861
671	0.048	921	0.634	0.860
672	0.048	922	0.637	0.861
673	0.048	923	0.640	0.861
674	0.048	924	0.640	0.860
675	0.048	925	0.641	0.861
676	0.048	926	0.643	0.860
677	0.049	927	0.645	0.860
678	0.049	928	0.650	0.861
679	0.049	929	0.660	0.862
680	0.050	930	0.660	0.859
681	0.050	931	0.658	0.858
682	0.051	932	0.658	0.857
683	0.052	933	0.652	0.853
684	0.053	934	0.642	0.848
685	0.054	935	0.628	0.843
			Avgndvi	0.858
			OptNDVI	0.852

---

NDVI LEVEL 4				
VISIBLE RED		NIR		NDVI
$\lambda(\text{nm})$	Reflectance	$\lambda(\text{nm})$	Reflectance	
650	0.047	900	0.647	0.864
651	0.047	901	0.645	0.864
652	0.047	902	0.644	0.865
653	0.046	903	0.645	0.867
654	0.045	904	0.645	0.870
655	0.045	905	0.653	0.872
656	0.044	906	0.658	0.875
657	0.043	907	0.661	0.877
658	0.043	908	0.656	0.876
659	0.043	909	0.652	0.877
660	0.042	910	0.649	0.878
661	0.042	911	0.647	0.879
662	0.041	912	0.646	0.880
663	0.041	913	0.649	0.882
664	0.041	914	0.648	0.882
665	0.040	915	0.647	0.883
666	0.040	916	0.646	0.884
667	0.040	917	0.646	0.884
668	0.039	918	0.647	0.885
669	0.039	919	0.639	0.885
670	0.039	920	0.636	0.885
671	0.039	921	0.639	0.885
672	0.039	922	0.645	0.886
673	0.039	923	0.652	0.887
674	0.039	924	0.653	0.887
675	0.039	925	0.655	0.887
676	0.039	926	0.657	0.887
677	0.040	927	0.667	0.887
678	0.040	928	0.676	0.888
679	0.040	929	0.682	0.888
680	0.042	930	0.696	0.887
681	0.042	931	0.707	0.887
682	0.043	932	0.696	0.884
683	0.044	933	0.677	0.878
684	0.045	934	0.654	0.870
685	0.047	935	0.637	0.863
			Avgndvi	0.880
			OptNDVI	0.820

---

NDVI LEVEL 3				
VISIBLE RED		NIR		NDVI
$\lambda(\text{nm})$	Reflectance	$\lambda(\text{nm})$	Reflectance	
650	0.062	900	0.544	0.796
651	0.061	901	0.546	0.798
652	0.061	902	0.547	0.80
653	0.060	903	0.550	0.804
654	0.059	904	0.555	0.808
655	0.059	905	0.560	0.811
656	0.058	906	0.560	0.813
657	0.057	907	0.559	0.814
658	0.058	908	0.556	0.812
659	0.057	909	0.554	0.812
660	0.057	910	0.552	0.813
661	0.057	911	0.550	0.813
662	0.056	912	0.548	0.814
663	0.055	913	0.546	0.815
664	0.056	914	0.546	0.815
665	0.056	915	0.547	0.815
666	0.055	916	0.546	0.816
667	0.055	917	0.548	0.817
668	0.055	918	0.550	0.818
669	0.055	919	0.551	0.818
670	0.055	920	0.552	0.8183
671	0.056	921	0.556	0.817
672	0.056	922	0.562	0.818
673	0.057	923	0.568	0.819
674	0.057	924	0.570	0.818
675	0.057	925	0.573	0.818
676	0.058	926	0.577	0.818
677	0.059	927	0.579	0.815
678	0.060	928	0.585	0.815
679	0.061	929	0.595	0.815
680	0.063	930	0.593	0.809
681	0.064	931	0.586	0.803
682	0.065	932	0.575	0.796
683	0.067	933	0.572	0.790
684	0.068	934	0.571	0.787
685	0.069	935	0.546	0.775
			Avgndvi	0.810
			OptNDVI	0.788

---

NDVI LEVEL 2				
VISIBLE RED		NIR		NDVI
$\lambda(\text{nm})$	Reflectance	$\lambda(\text{nm})$	Reflectance	
650	0.176	900	0.485	0.466
651	0.177	901	0.484	0.464
652	0.177	902	0.484	0.464
653	0.176	903	0.485	0.466
654	0.176	904	0.488	0.469
655	0.177	905	0.494	0.473
656	0.178	906	0.499	0.475
657	0.179	907	0.503	0.475
658	0.181	908	0.501	0.470
659	0.182	909	0.450	0.467
660	0.182	910	0.497	0.463
661	0.183	911	0.498	0.463
662	0.183	912	0.501	0.464
663	0.184	913	0.504	0.466
664	0.185	914	0.506	0.465
665	0.185	915	0.506	0.464
666	0.186	916	0.502	0.459
667	0.186	917	0.501	0.458
668	0.187	918	0.504	0.459
669	0.187	919	0.499	0.454
670	0.188	920	0.497	0.451
671	0.189	921	0.500	0.451
672	0.190	922	0.507	0.455
673	0.191	923	0.515	0.459
674	0.192	924	0.518	0.459
675	0.192	925	0.518	0.459
676	0.193	926	0.518	0.457
677	0.194	927	0.534	0.466
678	0.195	928	0.550	0.476
679	0.197	929	0.568	0.485
680	0.199	930	0.569	0.482
681	0.201	931	0.566	0.476
682	0.203	932	0.558	0.467
683	0.204	933	0.545	0.456
684	0.204	934	0.530	0.445
685	0.203	935	0.522	0.440
			Avgndvi	0.464
			OptNDVI	0.421

---

NDVI LEVEL 1				
VISIBLE RED		NIR		NDVI
$\lambda(\text{nm})$	reflectance	$\lambda(\text{nm})$	reflectance	
650	0.266	900	0.546	0.346
651	0.266	901	0.545	0.344
652	0.266	902	0.545	0.345
653	0.264	903	0.546	0.347
654	0.264	904	0.548	0.350
655	0.264	905	0.550	0.352
656	0.265	906	0.554	0.352
657	0.267	907	0.557	0.353
658	0.268	908	0.557	0.350
659	0.268	909	0.555	0.348
660	0.268	910	0.551	0.345
661	0.268	911	0.550	0.345
662	0.268	912	0.550	0.345
663	0.267	913	0.551	0.347
664	0.268	914	0.553	0.348
665	0.268	915	0.554	0.348
666	0.268	916	0.555	0.348
667	0.268	917	0.557	0.350
668	0.268	918	0.560	0.352
669	0.269	919	0.558	0.350
670	0.269	920	0.557	0.349
671	0.270	921	0.560	0.349
672	0.271	922	0.567	0.354
673	0.272	923	0.575	0.358
674	0.273	924	0.579	0.359
675	0.275	925	0.583	0.360
676	0.276	926	0.588	0.361
677	0.279	927	0.590	0.359
678	0.281	928	0.60	0.362
679	0.284	929	0.624	0.375
680	0.288	930	0.630	0.372
681	0.292	931	0.627	0.364
682	0.296	932	0.608	0.344
683	0.298	933	0.597	0.333
684	0.30	934	0.587	0.324
685	0.301	935	0.556	0.298
			Avgndvi	0.350
			OptNDVI	0.306

---

## B.2 Second set of Data, 4-14- 2004

NDVI LEVEL 6				
VISIBLE RED		NIR		NDVI
$\lambda(\text{nm})$	reflectance	$\lambda(\text{nm})$	reflectance	
650	0.02	900	0.43	0.911
651	0.02	901	0.429	0.911
652	0.02	902	0.427	0.910
653	0.02	903	0.427	0.910
654	0.02	904	0.428	0.911
655	0.02	905	0.427	0.910
656	0.02	906	0.428	0.911
657	0.019	907	0.428	0.915
658	0.019	908	0.428	0.915
659	0.019	909	0.428	0.915
660	0.02	910	0.429	0.911
661	0.019	911	0.431	0.916
662	0.019	912	0.432	0.916
663	0.019	913	0.432	0.916
664	0.019	914	0.431	0.916
665	0.019	915	0.431	0.916
666	0.019	916	0.431	0.916
667	0.019	917	0.428	0.915
668	0.019	918	0.424	0.914
669	0.019	919	0.425	0.914
670	0.019	920	0.426	0.915
671	0.019	921	0.427	0.915
672	0.019	922	0.427	0.915
673	0.019	923	0.426	0.915
674	0.02	924	0.424	0.910
675	0.02	925	0.424	0.910
676	0.02	926	0.426	0.910
677	0.02	927	0.425	0.910
678	0.02	928	0.425	0.910
679	0.02	929	0.426	0.910
680	0.021	930	0.43	0.907
681	0.021	931	0.432	0.907
682	0.022	932	0.425	0.902
683	0.022	933	0.425	0.902
684	0.023	934	0.429	0.898
685	0.023	935	0.418	0.896
			AvgNDVI	0.911
			OptNDVI	0.902

---

NDVI LEVEL 5				
VISIBLE RED		NIR		NDVI
$\lambda(\text{nm})$	reflectance	$\lambda(\text{nm})$	reflectance	
650	0.04	900	0.475	0.845
651	0.04	901	0.474	0.844
652	0.039	902	0.473	0.848
653	0.039	903	0.473	0.848
654	0.038	904	0.473	0.851
655	0.038	905	0.47	0.850
656	0.037	906	0.47	0.854
657	0.037	907	0.472	0.855
658	0.036	908	0.471	0.858
659	0.036	909	0.472	0.858
660	0.035	910	0.475	0.863
661	0.035	911	0.477	0.863
662	0.034	912	0.478	0.867
663	0.033	913	0.479	0.871
664	0.033	914	0.478	0.871
665	0.032	915	0.477	0.874
666	0.032	916	0.478	0.874
667	0.031	917	0.476	0.878
668	0.031	918	0.474	0.877
669	0.031	919	0.472	0.877
670	0.03	920	0.471	0.880
671	0.03	921	0.47	0.88
672	0.03	922	0.469	0.878
673	0.03	923	0.468	0.880
674	0.03	924	0.468	0.880
675	0.03	925	0.469	0.880
676	0.03	926	0.47	0.88
677	0.031	927	0.47	0.876
678	0.031	928	0.47	0.876
679	0.031	929	0.473	0.877
680	0.031	930	0.473	0.877
681	0.032	931	0.474	0.873
682	0.033	932	0.478	0.871
683	0.033	933	0.483	0.872
684	0.034	934	0.485	0.868
685	0.035	935	0.476	0.863
			AvgNDVI	0.868
			OptNDVI	0.869

---

NDVI LEVEL 4				
VISIBLE RED		NIR		NDVI
$\lambda(\text{nm})$	reflectance	$\lambda(\text{nm})$	reflectance	
650	0.067	900	0.525	0.774
651	0.066	901	0.526	0.777
652	0.065	902	0.526	0.780
653	0.065	903	0.524	0.779
654	0.065	904	0.522	0.778
655	0.064	905	0.523	0.782
656	0.064	906	0.524	0.782
657	0.063	907	0.524	0.785
658	0.062	908	0.526	0.789
659	0.061	909	0.528	0.793
660	0.06	910	0.528	0.796
661	0.059	911	0.528	0.799
662	0.058	912	0.53	0.803
663	0.057	913	0.532	0.806
664	0.056	914	0.533	0.810
665	0.055	915	0.532	0.813
666	0.054	916	0.532	0.816
667	0.054	917	0.53	0.815
668	0.053	918	0.526	0.817
669	0.053	919	0.527	0.817
670	0.052	920	0.526	0.820
671	0.052	921	0.525	0.820
672	0.051	922	0.525	0.823
673	0.051	923	0.524	0.823
674	0.051	924	0.523	0.823
675	0.051	925	0.523	0.823
676	0.051	926	0.524	0.823
677	0.051	927	0.526	0.823
678	0.051	928	0.527	0.823
679	0.052	929	0.527	0.820
680	0.052	930	0.53	0.821
681	0.053	931	0.533	0.819
682	0.054	932	0.532	0.816
683	0.055	933	0.536	0.814
684	0.057	934	0.541	0.809
685	0.058	935	0.538	0.805
				0.806
				0.814

NDVI LEVEL 3				
VISIBLE RED		NIR		NDVI
$\lambda(\text{nm})$	reflectance	$\lambda(\text{nm})$	reflectance	
650	0.094	900	0.554	0.710
651	0.093	901	0.555	0.713
652	0.092	902	0.554	0.715
653	0.091	903	0.555	0.718
654	0.09	904	0.555	0.721
655	0.089	905	0.554	0.723
656	0.088	906	0.554	0.726
657	0.086	907	0.554	0.731
658	0.084	908	0.554	0.737
659	0.083	909	0.554	0.739
660	0.081	910	0.554	0.745
661	0.079	911	0.558	0.752
662	0.077	912	0.56	0.758
663	0.075	913	0.56	0.764
664	0.074	914	0.559	0.766
665	0.072	915	0.558	0.771
666	0.071	916	0.559	0.775
667	0.07	917	0.558	0.777
668	0.069	918	0.553	0.778
669	0.068	919	0.553	0.781
670	0.067	920	0.553	0.784
671	0.066	921	0.553	0.787
672	0.066	922	0.554	0.787
673	0.067	923	0.555	0.785
674	0.067	924	0.558	0.786
675	0.067	925	0.557	0.785
676	0.068	926	0.553	0.781
677	0.069	927	0.555	0.779
678	0.07	928	0.558	0.777
679	0.071	929	0.561	0.775
680	0.073	930	0.562	0.770
681	0.075	931	0.561	0.764
682	0.077	932	0.559	0.758
683	0.08	933	0.563	0.751
684	0.083	934	0.568	0.745
685	0.087	935	0.551	0.727
			AvgNDVI	0.757
			OptNDVI	0.756

NDVI LEVEL 2				
VISIBLE RED		NIR		NDVI
$\lambda(\text{nm})$	reflectance	$\lambda(\text{nm})$	reflectance	
650	0.156	900	0.583	0.578
651	0.157	901	0.585	0.577
652	0.158	902	0.585	0.575
653	0.159	903	0.586	0.573
654	0.16	904	0.587	0.572
655	0.161	905	0.59	0.571
656	0.162	906	0.591	0.570
657	0.163	907	0.591	0.568
658	0.163	908	0.594	0.569
659	0.164	909	0.596	0.568
660	0.165	910	0.596	0.566
661	0.166	911	0.598	0.565
662	0.166	912	0.6	0.567
663	0.167	913	0.602	0.566
664	0.168	914	0.604	0.565
665	0.169	915	0.606	0.564
666	0.169	916	0.605	0.563
667	0.171	917	0.604	0.559
668	0.171	918	0.603	0.558
669	0.172	919	0.605	0.557
670	0.173	920	0.607	0.556
671	0.174	921	0.608	0.555
672	0.174	922	0.609	0.556
673	0.175	923	0.61	0.554
674	0.176	924	0.61	0.552
675	0.177	925	0.61	0.550
676	0.178	926	0.61	0.548
677	0.18	927	0.614	0.546
678	0.18	928	0.616	0.548
679	0.181	929	0.616	0.546
680	0.182	930	0.618	0.545
681	0.183	931	0.618	0.543
682	0.185	932	0.61	0.535
683	0.186	933	0.611	0.533
684	0.187	934	0.616	0.534
685	0.188	935	0.61	0.529
			Avgndvi	0.558
			OptNDVI	0.533

NDVI LEVEL 1				
VISIBLE RED		NIR		NDVI
$\lambda(\text{nm})$	reflectance	$\lambda(\text{nm})$	reflectance	
650	0.505	900	0.724	0.178194
651	0.507	901	0.725	0.176948
652	0.509	902	0.725	0.175041
653	0.51	903	0.725	0.174089
654	0.512	904	0.724	0.171521
655	0.514	905	0.724	0.169628
656	0.516	906	0.725	0.168413
657	0.518	907	0.725	0.166533
658	0.519	908	0.726	0.166265
659	0.521	909	0.727	0.165064
660	0.522	910	0.727	0.164131
661	0.524	911	0.729	0.163607
662	0.525	912	0.73	0.163347
663	0.527	913	0.73	0.161496
664	0.529	914	0.73	0.159651
665	0.53	915	0.729	0.158062
666	0.532	916	0.732	0.158228
667	0.534	917	0.73	0.155063
668	0.535	918	0.725	0.150794
669	0.536	919	0.725	0.149881
670	0.538	920	0.725	0.14806
671	0.541	921	0.728	0.14736
672	0.542	922	0.728	0.146457
673	0.543	923	0.727	0.144882
674	0.545	924	0.725	0.141732
675	0.546	925	0.727	0.142184
676	0.548	926	0.732	0.14375
677	0.55	927	0.733	0.142634
678	0.551	928	0.735	0.143079
679	0.552	929	0.739	0.144849
680	0.554	930	0.739	0.143078
681	0.556	931	0.739	0.141313
682	0.558	932	0.742	0.141538
683	0.559	933	0.746	0.143295
684	0.561	934	0.749	0.143511
685	0.562	935	0.752	0.144597
			AvgNDVI	0.155508
			OptNDVI	0.130164